Long-Range Electron Transfer in Porphyrin-Containing [2]-Rotaxanes: Tuning the Rate by Metal Cation Coordination

ARTICLE *in* JOURNAL OF THE AMERICAN CHEMICAL SOCIETY · APRIL 2002

Impact Factor: 12.11 · DOI: 10.1021/ja0119907 · Source: PubMed

J|A|C|S
ARTICLES
Published on Web 03/27/2002

Long-Range Electron Transfer in Porphyrin-Containing [2]-Rotaxanes: Tuning the Rate by Metal Cation Coordination

Mikael Andersson,† Myriam Linke,‡ Jean-Claude Chambron,‡ Jan Davidsson,† Valérie Heitz,‡ Leif Hammarström,*,† and Jean-Pierre Sauvage*,‡

Contribution from the Department of Physical Chemistry, Uppsala University, Box 532, S-751 21 Uppsala, Sweden, and Laboratoire de Chimie Organo-Minérale, UMR 7513 au C.N.R.S., Institut Le Bel, Université Louis Pasteur, 4, Rue Blaise Pascal, F-67070 Strasbourg, France

Received August 17, 2001. Revised Manuscript Received November 8, 2001

Abstract: A series of [2]-rotaxanes has been synthesized in which two Zn(II)-porphyrins (ZnP) electron donors were attached as stoppers on the rod. A macrocycle attached to a Au(III)-porphyrin (AuP^+) acceptor was threaded on the rod. By selective excitation of either porphyrin, we could induce an electron transfer from the ZnP to the AuP^+ unit that generated the same $ZnP^{\bullet+}$-$AuP^\bullet$ charge-transfer state irrespective of which porphyrin was excited. Although the reactants were linked only by mechanical or coordination bonds, electron-transfer rate constants up to 1.2×10^{10} s^{-1} were obtained over a 15−17 Å edge-to-edge distance between the porphyrins. The resulting charge-transfer state had a relatively long lifetime of 10−40 ns and was formed in high yield (>80%) in most cases. By a simple variation of the link between the reactants, viz. a coordination of the phenanthroline units on the rotaxane rod and ring by either Ag^+ or Cu^+, we could enhance the electron-transfer rate from the ZnP to the excited $^3AuP^+$. We interpret our data in terms of an enhanced superexchange mechanism with Ag^+ and a change to a stepwise hopping mechanism with Cu^+, involving the oxidized $Cu(phen)_2^{2+}$ unit as a real intermediate. When the ZnP unit was excited instead, electron transfer from the excited ^{1}ZnP to AuP^+ was not affected, or even slowed, by Ag^+ or Cu^+. We discuss this asymmetry in terms of the different orbitals involved in mediating the reaction in an electron- and a hole-transfer mechanism. Our results show the possibility to tune the rates of electron transfer between noncovalently linked reactants by a convenient modification of the link. The different effect of Ag^+ and Cu^+ on the rate with ZnP and AuP^+ excitation shows an additional possibility to control the electron-transfer reactions by selective excitation. We also found that coordination of the Cu^+ introduced an energy-transfer reaction from ^{1}ZnP to $Cu(phen)_2^+$ ($k = 5.1 \times 10^9$ s^{-1}) that proceeded in competition with electron transfer to AuP^+ and was followed by a quantitative energy transfer to give the ^{3}ZnP state ($k = 1.5 \times 10^9$ s^{-1}).

1. Introduction

In the photosynthetic reaction center of purple bacteria, photoinduced charge separation proceeds via a series of electron-transfer steps between porphyrin-like components and quinones.[1] The reactant molecules are held together by the protein without being covalently linked. In general, the electronic coupling between electron donor and acceptor molecules is mediated by the intervening medium to different extents, depending on its electronic structure. Extensive studies of synthetic model systems with a variable reactant distance have demonstrated the efficiency of through-bond mediation,[2] in particular through covalent bonds. A protein medium has a more complicated structure. Multiple electron-transfer pathways may exist, comprising covalent bonds, hydrogen bonds, space jumps, etc.[3] Small structural changes in the protein could affect the electronic coupling along the different paths, thereby controlling the rate of the electron-transfer reactions. As an example, evidence has been found that the second quinone acceptor, Q_B, of purple bacterial reaction centers moves ca. 4.5 Å upon the first reduction,[4] which is probably important for subsequent reaction steps. Also, in cytochrome bc_1 large motions of the [2Fe2S] domain have been shown necessary for the electron-transfer

* To whom correspondence should be addressed. L.H.: Leifh@fki.uu.se. J.-P.S.: sauvage@chimie.u-strasbg.fr.
† Uppsala University.
‡ Université Louis Pasteur.

(1) (a) *Anoxygenic Photosynthetic Bacteria*; Blankenship, R. E., Madigan, M. T., Bauer, C. E., Eds.; Kluwer Academic Publishers: Dordrecht, 1995. (b) Diesenhofer, J.; Michel, H. *Angew. Chem., Int. Ed. Engl.* **1989**, *28*, 829. (c) Huber, R. *Angew. Chem., Int. Ed. Engl.* **1989**, *28*, 848.
(2) (a) Oevering, H.; Paddon-Row, M. N.; Heppener, M.; Oliver, A. M.; Cotsaris, E.; Verhoeven, J. W.; Hush, N. S. *J. Am. Chem. Soc.* **1987**, *109*, 3258. (b) Johnson, M. D.; Miller, J. R.; Green, N. S.; Closs, G. L. *J. Phys. Chem.* **1989**, *93*, 1173. (c) Helms, A.; Heiler, D.; McLendon, G. *J. Am. Chem. Soc.* **1992**, *114*, 6227. (d) Finckh, P.; Heitele, H.; Volk, M.; Michel-Beyerle, M. E. *J. Phys. Chem.* **1988**, *92*, 6584. (e) Ribou, A. C.; Launay, J. P.; Takahashi, K.; Nihira, T.; Tarutani, S.; Spangler, C. W. *Inorg. Chem.* **1994**, *33*, 1325. (f) Wasielewski, M. R.; Johnsson, D. G.; Svec, W. A.; Kersey, K. M.; Cragg, D. F.; Minsek, D. W. In *Photochemical Energy Conversion*; Norris, J. R., Meisel, D., Eds.; Elsevier: New York, 1989.
(3) For different opinions, see: (a) Beratan, D. N.; Betts, J. N.; Onuchic, J. N. *Science* **1991**, *252*, 1285. (b) Beratan, D. N.; Onuchic, J. N.; Winkler, J. R.; Gray, H. B. *Science* **1992**, *258*, 1740. (c) Gray, H. B.; Winkler, J. R. *Annu. Rev. Biochem.* **1996**, *65*, 537. (d) Moser, C. C.; Keske, J. M.; Warncke, K.; Farid, R. S.; Dutton, L. *Nature* **1992**, *355*, 796. (e) Page, C. C.; Moser, C. C.; Xiaoxi, C.; Dutton, L. *Nature* **1999**, *402*, 47.
(4) Stowell, M. H. B.; McPhillips, T. M.; Rees, D. C.; Soltis, S. M.; Abresch, E.; Feher, G. *Science* **1997**, *276*, 812.

function of the protein.[5] However, for electron transfer over longer distances, additional redox cofactors or redox active amino acid residues such as tyrosine often act as real intermediates in a charge-hopping mechanism,[3e] to reach sufficient rates. There is currently a great interest in the mediation mechanism in different systems[6−8] and the distinction between superexchange[9] and a charge-hopping mechanism. In a superexchange, the mediating states of the link only induce a small perturbation, while in a hopping mechanism, the intermediates are transiently populated which can lead to a very efficient electron transfer over long distances.[6−8]

In contrast to the case in proteins, relatively few synthetic systems exhibiting long-range electron transfer have employed links other than covalent links to assemble the donor and acceptor. Hydrogen bonds have attracted attention for this purpose[10] due to their possible importance in proteins, and also coordination bonds have been employed.[11] Recently, donor/acceptor interactions and pure mechanical links have been used.[13] Also, a few of these systems have used molecular mobility to enhance charge separation and suppress back reactions.

In the present paper, we present a series of [2]-rotaxanes (Figure 4) that exhibits photoinduced electron transfer between Zn(II)-porphyrin (ZnP) and Au(III)-porphyrin (AuP^+) units. Rotaxanes are described as a ring threaded on a rod with stoppers that prevent dissociation. In the present case, the ZnP electron donors also act as stoppers on the rod, and the AuP^+ acceptor is attached to the ring. Thus, in $\mathbf{Zn_2//Au^+}$ the redox active porphyrins are held together only by mechanical bonds, and no covalent electron-transfer pathway exists. By binding different metal cations to the phenanthrolines, forming $\mathbf{Zn_2/Ag^+/Au^+}$, $\mathbf{Zn_2/Cu^+/Au^+}$, and $\mathbf{Zn_2/Li^+/Au^+}$, the rod and ring become connected by coordination bonds. There is no readily identifiable single pathway for electron transfer between the ZnP and AuP^+ units, and all possible pathways include link segments with different electronic structure and a jump through space

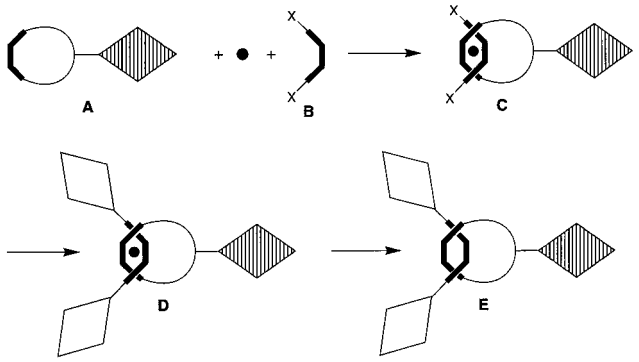

Figure 1. Principle of transition metal-templated synthesis of a [2]-rotaxane. A thick line represents a dpp chelate, a black dot represents a metal cation, a hatched diamond represents a Au(III) porphyrin, and an empty diamond represents a Zn(II) porphyrin. The transition metal controls the threading of Au(III) porphyrin-pendant macrocycle **A** onto chelate **B**, to form prerotaxane **C**. Construction of the porphyrin stoppers at the X functions leads to the metal complex [2]-rotaxane **D**. Removal of the template cation forms the free rotaxane **E**.

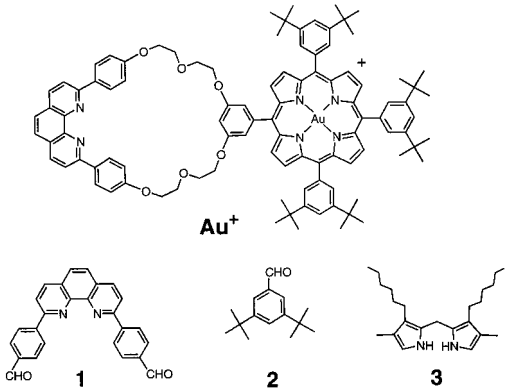

Figure 2. Precursors to the synthesis of [2]-rotaxanes.

and/or coordination bonds, somewhat resembling the case in proteins. Some mobility of the rotaxane units is also possible, which might affect the electron-transfer rates.

The aim of this study was to investigate the possibility of enhancing the electron-transfer rates by coordination of the metal cations and to compare the effects of space jumps versus metal−ligand bonds in the electron-transfer pathway. Coordination of the metal cations will increase the electronic coupling between the phenanthrolines considerably, change the energy of their molecular orbitals, and also introduce new, metal-based orbitals. Thus, if the electron-transfer pathway involves the metal-phenanthroline complex moiety, one would expect a significant increase in reaction rate.

Both the ZnP and the AuP^+ units can be selectively excited, so that electron transfer can be initiated from different excited states. In both cases the product is the $ZnP^{\bullet+}$-$AuP^{\bullet}$ charge-transfer state. When ZnP was excited, we did not observe any effect of the Ag^+ or Cu^+ cations on the electron-transfer reaction. Interestingly, however, when AuP^+ was excited Ag^+ increased the electron-transfer rate, which we have reported in a previous communication.[13] We interpreted this as a superexchange mediation involving the $Ag(phen)_2^+$ unit, that is enhanced as compared to the case in $\mathbf{Zn_2//Au^+}$. In the present paper, we have expanded the series of rotaxanes and found that with Cu^+, the rate was further increased, and the reaction presumably involved the oxidized $Cu(phen)_2^{2+}$ complex as a real intermediate. Thus, we propose that the role of the metal-

(5) Darrouzet, E.; Valkova-Valchanova, M.; Moser, C. C.; Dutton, L.; Daldal, F. *Proc. Natl. Acad. Sci. U.S.A.* **2000**, *97*, 4567.
(6) Bixon, M.; Jortner, J. *Adv. Chem. Phys.* **1999**, *106*, 35.
(7) Davis, W. B.; Svec, W. A.; Ratner, M. A.; Wasielewski, M. R. *Nature* **1998**, *396*, 60.
(8) (a) Lewis, F. D.; Liu, X.; Liu, J.; Miller, S. E.; Hayes, R. T.; Wasielewski, M. R. *Nature* **2000**, *406*, 51. (b) Schuster, G. B. *Acc. Chem. Res.* **2000**, *33*, 253. (c) Bixon, M.; Giese, B.; Wessely, S.; Langenbacher, T.; Michel-Beyerle, M. E.; Jortner, J. *Proc. Natl. Acad. Sci. U.S.A.* **1999**, *96*, 11713. (d) Meggers, E.; Michel-Beyerle, M. E., Giese, B. *J. Am. Chem. Soc.* **1998**, *120*, 12950. (e) Lewis, F. D.; Wu, T.; Zhang, Y.; Letsinger, R. L.; Greenfield, S. R.; Wasielewski, M. R. *Science* **1997**, *277*, 673.
(9) McConnell, H. M. *J. Chem. Phys.* **1961**, *35*, 508.
(10) (a) Turro, C.; Chang, C. K.; Leroi, G. E.; Cukier, R. I.; Nocera, D. G. *J. Am. Chem. Soc.* **1992**, *114*, 4013. (b) Berman, A.; Izraeli, E. S.; Levanon, H.; Wang, B.; Sessler, J. L. *J. Am. Chem. Soc.* **1995**, *117*, 8252. (c) Kirby, J. P.; Roberts, J. A.; Nocera, D. G. *J. Am. Chem. Soc*. **1997**, *119*, 9230. (d) Yang, J.; Seneviratne, D.; Arbatin, G.; Andersson, A. M.; Curtis, J. C. *J. Am. Chem. Soc*. **1997**, *119*, 5329. (e) Harriman, A.; Kubo, Y.; Sessler, J. L. *J. Am. Chem. Soc*. **1992**, *114*, 388. (f) Cukier, R. I.; Nocera, D. G. *Annu. Rev. Phys. Chem*. **1998**, *49*, 337. Ghaddar, T. H.; Castner, E. W.; Isied, S. *J. Am. Chem. Soc*. **2000**, *122*, 1233. (g) Osuka, A.; Yoneshima, R.; Shiratori, H.; Okada, T.; Taniguchi, S.; Mataga, N. *Chem. Commun*. **1998**, 1567.
(11) (a) Harriman, A.; Sauvage, J.-P. *Chem. Soc. Rev*. **1996**, 41. (b) Harriman, A.; Ziessel, R. *Chem. Commun*. **1996**, 1707. (c) Dixon, I. M.; Collin, J. P.; Sauvage, J.-P.; Barigelletti, F.; Flamigni, L. *Angew. Chem., Int. Ed.* **2000**, *39*, 1292. (d) Imahori, H.; Yoshizawa, E.; Yamada, K.; Hagiwara, K.; Okada, T.; Sakata, Y. *J. Chem. Soc., Chem. Commun*. **1995**, *11*, 1133.
(12) (a) Linke, M.; Chambron, J.-C.; Heitz, V.; Sauvage, J.-P. *J. Am. Chem. Soc.* **1997**, *119*, 11329. (b) Ashton, P. R.; Balzani, V.; Kocian, O.; Prodi, L.; Spencer, N.; Stoddart, J. F. *J. Am. Chem. Soc.* **1998**, *120*, 11190. (c) Hu, Y.-Z.; Bossmann, S. H.; van Loyen, D.; Schwartz, O.; Dürr, H. *Chem.-Eur. J.* **1999**, *5*, 1267. (d) Hu, Y.-Z.; Tsukiji, S.; Shinkai, S.; Oishi, S.; Dürr, H.; Hamachi, I. *Chem. Lett.* **2000**, 442.
(13) Andersson, M.; Linke, M.; Chambron, J.-C.; Davidsson, J.; Heitz, V.; Sauvage, J.-P.; Hammarström, L. *J. Am. Chem. Soc*. **2000**, *122*, 3526.

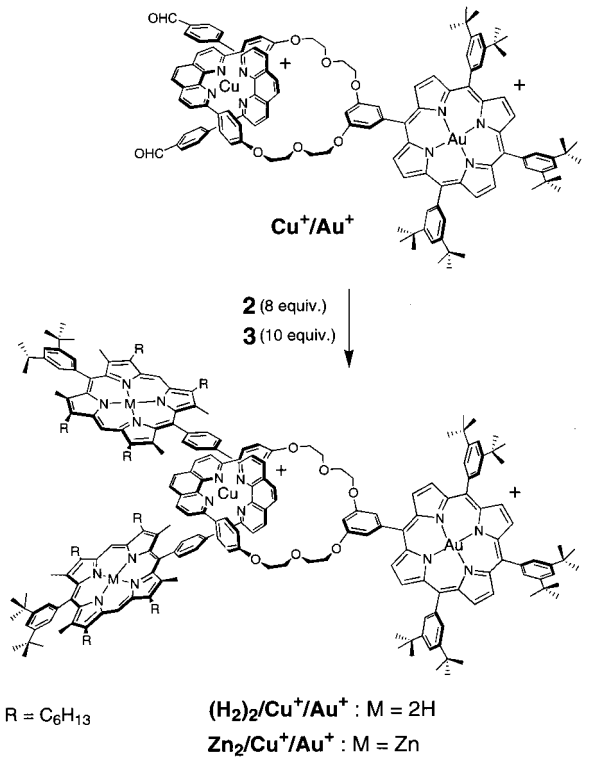

Figure 3. Synthesis of $(H_2)_2/Cu^+/Au^+$.

phenanthroline complex changes from that of an efficient superexchange mediator in the case of Ag^+ to an intermediate site in a rapid charge-hopping mechanism in the case of Cu^+. We also propose that the different mediation effects with ZnP and AuP^+ excitation can be rationalized by the involvement of different mediating orbitals, that is, an "electron-transfer"[2b,6,14] pathway with ZnP excitation but "hole-transfer"[2b,6,14] with AuP^+ excitation. A complete account of our photochemical results is given, including the subsequent recombination and ZnP triplet reactions as well as data for three new rotaxanes. Furthermore, the synthesis and structural characterization of the series of rotaxanes are described.

2. Results and Discussion

2.1. Design and Synthesis. Principle of Rotaxane Construction. Rotaxanes made of a pendant gold-porphyrin macrocycle threaded inside a bis-zinc porphyrin stoppered dumbbell are built using a template approach to assemble the two parts of the system, the dumbbell and the macrocycle. This has already led to the synthesis of various catenanes,[15] rotaxanes,[16] and knots.[17] The principle of template construction is depicted in Figure 1. The precursor **C** to the rotaxane **E** called prerotaxane is obtained in one step from a gold porphyrin macrocycle **A** and a difunctionalized thread **B**, thanks to the gathering properties of a transition metal (black dot). Construction of the porphyrin blocking groups is the kinetically templated key step leading to the metal-complexed rotaxane structure **D**. The desired rotaxane **E** is obtained after removal of the metal template from **D**.

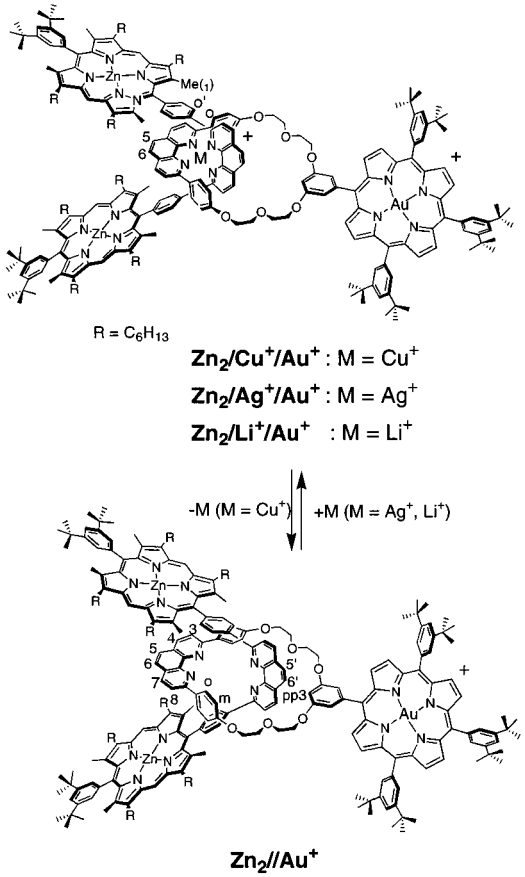

Figure 4. Illustration of the demetalation/remetalation reactions carried out on the Cu(I)-complexed [2]-rotaxane $Zn_2/Cu^+/Au^+$ to afford free [2]-rotaxane $Zn_2//Au^+$ and metallo-[2]-rotaxanes $Zn_2/Ag^+/Au^+$ and $Zn_2/Li^+/Au^+$. In the free [2]-rotaxane $Zn_2//Au^+$, the macrocycle is more deeply buried inside the cavity formed by the bis-porphyrin dumbbell as compared to the complexed [2]-rotaxanes.

Synthesis of [2]-Rotaxanes. The precursors to the synthesis of [2]-rotaxanes are represented in Figure 2. The macrocycle Au^+ bearing a 2,9-diphenyl-1,10-phenanthroline chelate (dpp) and a pendant gold(III) porphyrin was synthesized and used as a building block for the construction of porphyrin-containing [2]-catenanes.[18] Mixing Au^+ with equimolar amounts of $Cu(CH_3CN)_4PF_6$[19] followed by addition of 2,9-di(*p*-formylphenyl)-1,10-phenanthroline[20] **1** gave quantitatively the prerotaxane Cu^+/Au^+. This copper(I) complex was submitted to porphyrin synthesis[21] at the aldehyde function by reaction with 3,5-di-*tert*-butylbenzaldehyde **2** (8 equiv),[22] (3,3′-dihexyl-4,4′dimethyl-2,2′-dipyrryl)methane (10 equiv) **3**, and a few drops of

(14) Newton, M.*Chem. Rev.* **1991**, *91*, 767.
(15) (a) Dietrich-Buchecker, C.; Sauvage, J.-P. *Chem. Rev.* **1987**, *87*, 795. (b) Dietrich-Buchecker, C.; Sauvage, J.-P. *Tetrahedron* **1990**, *46*, 503. (c) Sauvage, J.-P. *Acc. Chem. Res.* **1990**, *23*, 327.
(16) (a) Chambron, J.-C.; Heitz, V.; Sauvage, J.-P. *J. Chem. Soc., Chem. Commun.* **1992**, 1131. (b) Chambron, J.-C.; Heitz, V.; Sauvage, J.-P. *J. Am. Chem. Soc.* **1993**, *115*, 12378.
(17) (a) Dietrich-Buchecker, C. O.; Sauvage, J.-P. *Angew. Chem., Int. Ed. Engl.* **1989**, *28*, 189. (b) Dietrich-Buchecker, C. O.; Sauvage, J.-P.; Kintzinger, J.-P.; Maltèse, P.; Pascard, C.; Guilhem, J. *New J. Chem.* **1992**, *16*, 931. (c) Dietrich-Buchecker, C. O.; Nierengarten, J.-F.; Sauvage, J.-P.; Armaroli, N.; Balzani, V.; De Cola, L. *J. Am. Chem. Soc.* **1993**, *115*, 11237. (d) Carina, R.; Dietrich-Buchecker, C.; Sauvage, J.-P. *J. Am. Chem. Soc.* **1996**, *118*, 9110. (e) Dietrich-Buchecker, C. O.; Sauvage, J.-P.; De Cian, A.; Fischer, J. *J. Chem. Soc., Chem. Commun.* **1994**, 2231.
(18) (a) Amabilino, D. B.; Sauvage, J.-P. *Chem. Commun.* **1996**, 2441−2442. (b) Amabilino, D. B.; Sauvage, J.-P. *New. J. Chem.* **1998**, *22*, 395.
(19) Kubas, G. J.; Monzyk, B.; Crumbliss, A. L. *Inorg. Synth.* **1990**, *28*, 90.
(20) Linke, M.; Chambron, J.-C.; Heitz, V.; Sauvage, J.-P.; Encinas, S.; Barigelletti, F.; Flamigni, L. *J. Am. Chem. Soc.* **2000**, *122*, 11834.
(21) (a) Lindsey, J. S.; Hsu, H. C.; Schreiman, I. C. *Tetrahedron Lett.* **1986**, *27*, 4969. (b) Lindsey, J. S.; Schreiman, I. C.; Hsu, H. C.; Kearney, P. C.; Marguerettaz, A. M. *J. Org. Chem.* **1987**, *52*, 827. (c) Lindsey, J. S.; Wagner, R. W. *J. Org. Chem.* **1989**, *54*, 828.
(22) Chardon-Noblat, S.; Sauvage, J.-P. *Tetrahedron* **1991**, *47*, 5123.

Table 1. Selected ^{1}H NMR Data for the Rotaxanes and Reference Compounds[a]

	dumbbell protons							macrocycle protons								
compound	meso	5′,6′	4′,7′	3′,8′	o′	m′	Me1	py1	py2	5,6	4,7	3,8	o	m	pp3	op3
Cu$^+$/Au$^+$	9.69[b]	8.46	8.94	8.11	7.67	7.12		9.44	9.29	7.84	8.43	7.91	7.22	6.12	7.33	7.59
(H$_2$)$_2$/Cu$^+$/Au$^+$	10.16	8.86	9.21	8.52	8.07	7.46	1.78	9.55	9.45	7.54	8.32	8.06	7.60	6.33	7.21	7.63
Zn$_2$/Cu$^+$/Au$^+$	10.12	8.86	9.27	8.54	8.07	7.47	1.76	9.56	9.45	9.55	8.26	8.04	7.58	6.35	7.20	7.67
Zn$_2$/Ag$^+$/Au$^+$	10.09	8.77	9.38	8.58	8.09	7.54	1.70	9.54	9.44	7.33	8.14	7.52	7.76	6.45	7.16	7.62
Zn$_2$/Li$^+$/Au$^+$	10.11	8.89	9.21	8.48	7.97	7.44	1.75	9.56	9.45	7.39	8.23	8.12	7.58	6.36	7.19	7.63
Zn$_2$/Au$^+$	10.03	7.98	8.57	8.90	9.48	7.72	2.03	9.42	9.24	4.85	6.72	7.53	8.63	7.00	7.86	7.70

[a] Chemical shifts in ppm downfield from TMS. Solvent: CD_2Cl_2. [b] C*H*O proton.

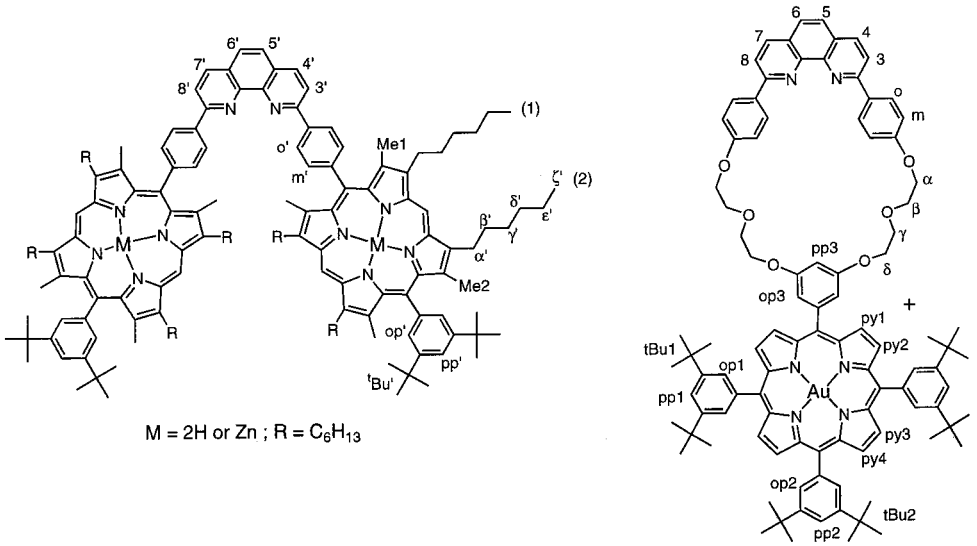

Figure 5. Numbering of protons for the two components of a [2]-rotaxane, the bis-porphyrin dumbbell, and the gold(III)-porphyrin-pendant macrocycle.

trifluoroacetic acid in CH_2Cl_2 (Figure 3). The mixture was stirred at room temperature for 16 h. After addition of tetrachloro-*p*-benzoquinone to oxidize the intermediate porphyrinogen groups formed, the mixture was refluxed for 1.5 h. The crude product was subjected to chromatographic purifications on silicagel, which resulted in 18% isolated yield of the free base copper(I) [2]-rotaxane **(H$_2$)$_2$/Cu$^+$/Au$^+$**. Complexation of the porphyrin stoppers was achieved by reacting **(H$_2$)$_2$/Cu$^+$/Au$^+$** for 1 h with 2 equiv of $Zn(OAc)_2 \cdot 2H_2O$ in a refluxing mixture of $CHCl_3$ and CH_3OH. The **Zn$_2$/Cu$^+$/Au$^+$** [2]-rotaxane was obtained in 82% yield.

To remove the copper template, a solution of **Zn$_2$/Cu$^+$/Au$^+$** was reacted with 50 equiv of KCN in a ternary mixture of $CHCl_3/H_2O/CH_3CN$ (1/1/4).[23] Demetalation did not go further after refluxing the solution for 30 min; therefore, the metal-free [2]-rotaxane was separated by column chromatography, and the remaining **Zn$_2$/Cu$^+$/Au$^+$** was subjected to the same reaction again. This procedure was repeated five times to lead to the free rotaxane **Zn$_2$//Au$^+$** in 92% yield.

Coordination Chemistry Performed on the dpp Chelates of the [2]-Rotaxane Zn$_2$//Au$^+$. The free coordination site formed by the dpp chelate can be occupied by other metals accommodating a tetrahedral geometry. Thus, treating the free **Zn$_2$//Au$^+$** rotaxane with lithium or silver salt resulted quantitatively in the formation of two new complexed rotaxanes, **Zn$_2$/Li$^+$/Au$^+$** and **Zn$_2$/Ag$^+$/Au$^+$** (Figure 4). These complexes have a conformation similar to the **Zn$_2$/Cu$^+$/Au$^+$** complex. They have been characterized by mass spectroscopy, ^{1}H NMR spectroscopy, and in the case of **Zn$_2$/Li$^+$/Au$^+$**, also by ^{7}Li NMR spectroscopy.

2.2. Conformation of the Different [2]-Rotaxanes Studied by NMR Spectroscopy. Relevant protons, which can be considered as probes for the geometry of the different [2]-rotaxanes, are reported in Table 1. The proton labeling of the components of these rotaxanes is shown in Figure 5. The ^{1}H NMR spectrum of prerotaxane **Cu$^+$/Au$^+$** was discussed in a previous paper and is in agreement with an extended conformation of this molecule.[18b] Introduction of the porphyrin stoppers led to a downfield shift of the protons localized on the thread of **(H$_2$)$_2$/Cu$^+$/Au$^+$** due to the deshielding effects exerted by the porphyrin rings. Zinc coordination on both porphyrins results in almost no change in the chemical shift of **Zn$_2$/Cu$^+$/Au$^+$** as compared to that of **(H$_2$)$_2$/Cu$^+$/Au$^+$**. The postulated conformation of **Zn$_2$/Cu$^+$/Au$^+$**, an extended one, in which the two zinc porphyrins and the gold porphyrin are as far as possible from each other is supported by several dipolar correlations observed on 2-D ROESY spectra. For example, protons o located on the macrocycle correlate both with protons o′ and with Me(1) of the dumbbell (Figure 4).

Exchanging either Li$^+$ or Ag$^+$ for Cu$^+$ led to similar ^{1}H NMR spectra. In the case of **Zn$_2$/Ag$^+$/Au$^+$**, a downfield shift of 0.5 ppm for protons m and 3,8 of the macrocycle is observed. This may result from the larger size of the Ag$^+$ cation, which would move the dpp chelate away from the shielding field of the other chelate. In the case of the lithium rotaxane **Zn$_2$/Ag$^+$/Au$^+$**, the chemical shift of the lithium is 2.79 ppm, a value close to the chemical shift of lithium in the lithium (I) [2]-catenane (δ =

(23) (a) Albrecht-Gary, A.-M.; Saad, Z.; Dietrich-Buchecker, C. O.; Sauvage, J.-P. *J. Am. Chem. Soc.* **1985**, *107*, 3205. (b) Dietrich-Buchecker, C. O.; Sauvage, J.-P.; Kern, J.-M. *J. Am. Chem. Soc.* **1984**, *106*, 3043.

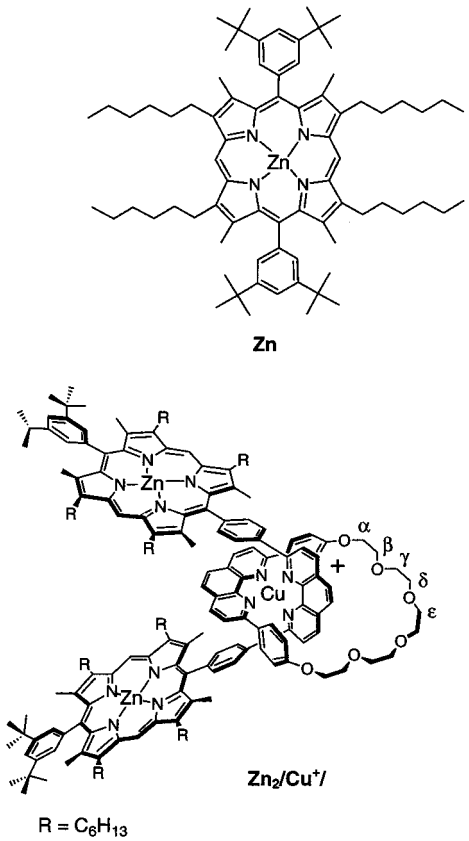

Figure 6. Structures of the model compounds **Zn** and **Zn_2/Cu^+/**.

2.2 ppm).[24] This result was a good proof of the presence of lithium coordinated by the two dpp chelate in **$Zn_2/Li^+/Au^+$**.

Removal of the copper template resulted in some important modifications of the **$Zn_2//Au^+$** spectra, explained by a less constrained molecule in which the macrocycle has moved toward the cavity formed by the bis-porphyrin thread. Thus, the phenanthroline protons (5,6), (4,7), and (3,8) now lie in the shielding field of the two zinc porphyrins and are shielded by −2.7, −1.94, and −0.51 ppm, respectively. Protons o and m that do not experience the phenanthroline field anymore are deshielded by +1.05 and +0.65 ppm, respectively. This new conformation is supported by dipolar coupling observed between proton m and both Me(1) and o′. Other important chemical shifts resulting from demetalation are the upfield shift of protons 5′,6′ (−0.88 ppm) and 4′,7′ (−0.80 ppm)and the deshielding of proton pp3 (0.66 ppm). A folding of the macrocycle placing the gold porphyrin macrocycle above the dpp fragment of the dumbbell can be proposed to account for these observations.

2.3. Photophysics and Photochemistry. The photoinduced reactions in the rotaxanes **$Zn_2/Cu^+/Au^+$**, **$Zn_2/Ag^+/Au^+$**, and **$Zn_2//Au^+$** of Figure 4 were studied with time-resolved emission and transient absorption spectroscopy. (The results from **$Zn_2/Li^+/Au^+$** are not included here because of the instability of this Li^+ complex in DMF, the solvent used for the photophysical experiments.) Model compounds were macrocycle **Au^+** with attached gold(III) porphyrin (Figure 2), Zn(II) porphyrin **Zn**, and Cu(I)-complexed [2]-rotaxane **Zn_2/Cu^+/** lacking the appended Au(III) porphyrin (Figure 6). The reactions in the rotaxanes are discussed starting with those initiated from the fluorescent ^{1}ZnP singlet excited state and continuing with those initiated from the nonemitting $^3AuP^+$ triplet state.

Table 2. Electrochemical Potentials[a] and Excited State Energies

reference compound[b] or component[c]	E_{ox} (V vs SCE)	E_{red} (V vs SCE)	^1E (eV)	^3E (eV)
AuP^+	1.6[d]	−0.52 (−0.55)	2.18	1.75
ZnP	0.70 (0.71)	−1.55[e]	2.13	1.72
/Cu/	(1.00)	−1.50[f]		1.85[e]
$Ag(dpp)_2^+$	∼1.5[d]	−0.7[g]	>3[h]	2.49[e]

[a] See Figures S3 and S4. [b] The reference compounds are **Zn**, **Au^+**, and $Ag(dpp)_2^+$, and /Cu/ denotes the $Cu(dpp)_2^+$ component of the [2]-rotaxane **$Zn_2/Cu^+/Au^+$**. [c] The numbers in brackets are determined for the corresponding components in the [2]-rotaxane **$Zn_2/Cu^+/Au^+$**. [d] Reference 43c. [e] Reference 36. [f] Value for related unit, refs 28, 39. [g] Reference 43a. [h] Reference 46.

2.3.1. Properties of the Individual Porphyrin Components. The absorption spectra of the rotaxanes were equal to a sum of the spectra of the model porphyrins **Zn** and **Au^+** (Supporting Information, Figure S1), indicating that the electronic coupling between the porphyrins is very weak. The spectra show that the ZnP units can be excited at 575 nm with a >90% selectivity, while a 70% selectivity of the AuP^+ excitation is achieved at 528 nm. The excited-state energies and redox potentials of the ZnP and AuP^+ units are given in Table 2. The lifetime of the excited singlet state of **Zn** was 2.0 ns, as determined from the fluorescence lifetime. In similar Zn(II)-porphyrins the ^{1}ZnP state is converted to the triplet ^{3}ZnP state with a yield of 0.8−0.9.[25−27] From transient absorption measurements of the ^{3}ZnP state of **Zn**, a lifetime of 7.5 μs was obtained. The lowest excited singlet state of the AuP^+ units undergoes a rapid intersystem crossing within a few picoseconds,[25,28,29] due to strong spin−orbit coupling. Thus, the electron-transfer reactions induced by AuP^+ excitation started from the $^3AuP^+$ state. The lifetime of this state in **Au^+** was 2.0 ns, as determined from the decay of its transient absorption.

Zn(II)-tetraphenyl and -octaethyl porphyrins usually have triplet lifetimes of 0.1−1 ms[25−28] in deoxygenated solutions, which is much longer than the value observed here. However, in a recent publication,[27a] similarly short triplet lifetimes were measured for mono- and di-meso-phenyl-substituted ZnOEP. It was suggested that steric interaction between the phenyl and alkyl substituents induced a conformational change to a nonplanar porphyrin in the triplet state, leading to a more rapid relaxation to the ground state. In our transient absorption spectra of the triplet state of **Zn**, we noted a shift of the transient absorption maximum from 454 to 462 nm, with isosbestic points at 460 and 510 nm, consistent with a conversion between two triplet states. From the transient absorption kinetics, we found that this conversion occurred with a time constant of 100 ns.

(24) Dietrich-Buchecker, C. O.; Sauvage, J.-P.; Kern, J.-M. *J. Am. Chem. Soc.* **1989**, *111*, 7791.
(25) Kalyanasundaran, K. *Photochemistry of Polypyridine and Porphyrin Complexes*; Academic Press: London, 1992.
(26) (a) Kalyanasundaran, K.; Neumann-Spallert, M. *J. Phys. Chem.* **1982**, *86*, 5163. (b) Flamigni, L.; Armaroli, N.; Barigelletti, F.; Balzani, V.; Collin, J.-P.; Dalbavie, J.-O.; Heitz, V.; Sauvage, J.-P. *J. Phys. Chem. B* **1997**, *101*, 5936.
(27) (a) Knyukshto, V.; Zenkevich, E.; Sagun, E.; Shulga, A.; Bachilo, S. *Chem. Phys. Lett.* **1998**, *297*, 97. (b) Darwent, J. R.; Douglas, P.; Harriman, A.; Porter, G.; Richoux, M.-C. *Coord. Chem. Rev.* **1982**, *44*, 83. (c) Tran-Thi, T. H.; Desforge, C.; Thiec, C.; Gaspard, S. *J. Phys. Chem.* **1989**, *93*, 1226. (d) Gouterman, M. In *The Porphyrins*; Dolphin, D., Ed.; Academic Press: New York, 1978; Vol. 3.
(28) Brun, A. M.; Harriman, A.; Heitz, V.; Sauvage, J.-P. *J. Am. Chem. Soc.* **1991**, *113*, 8657.
(29) Antipas, A.; Dolphin, D.; Gouterman, M.; Johnson, E. C. *J. Am. Chem. Soc.* **1978**, *100*, 7705.

Table 3. Summary of Forward Electron-Transfer Rate Constants, Calculated as $k_{ET} = 1/\tau - 1/\tau_0$, Where τ and τ_0 Are the Excited State Lifetimes in the Rotaxane and Model Compounds

	k_{ET} (s^{-1}) (rel. amplitudes)			
	ZnP excitation		AuP^+ excitation	
$\mathbf{Zn_2//Au^+}$	1.2×10^{10} (35%)	1.3×10^{9} (65%)	1.1×10^{10} (40%)	5×10^{8} (60%)
$\mathbf{Zn_2/Ag^+/Au^+}$	1.2×10^{10} (35%)	1.1×10^{9} (65%)	2.0×10^{10} (40%)	2.0×10^{9} (60%)
$\mathbf{Zn_2/Cu^+/Au^+}$	1.2×10^{10} [a]	*a*	3.9×10^{10} (75%)	1.6×10^{9} (25%)

[a] See text.

Similar data have recently been presented for Zn(II)-di-meso-diaryloctaalkyl porphyrins.[30] Thus, it seems that a conversion $^3ZnP_{initial} \rightarrow {}^3ZnP_{distorted}$ occurs with a lifetime of 100 ns in these porphyrins, leading to a substantial reduction in the intrinsic triplet lifetime. In donor/acceptor assemblies involving this type of Zn(II)-porphyrins, the unusually short lifetimes should thus not be misinterpreted as indicating any interaction between the ^{3}ZnP and other intramolecular components. In the present work, we monitored the electron-transfer reactions on the nanosecond time scale at 460 nm (the isosbestic point), to avoid any interference from the triplet dynamics.

2.3.2. Reactions in $\mathbf{Zn_2//Au^+}$. Excitation of the ZnP Unit. Selective excitation at 575 nm initially created the lowest excited singlet state of a ZnP unit. The ^{1}ZnP fluorescence intensity in $\mathbf{Zn_2//Au^+}$ was quenched by 88.5% as compared with the model **Zn**. Also the lifetime of the fluorescence was reduced. A double exponential fit gave lifetimes of 80 ps (35%) and 570 ps (65%), which should be compared with 2.0 ns for **Zn**. The reduction in lifetime was due to electron transfer between the ^{1}ZnP and AuP^+ units, forming a charge-transfer state:

$$\mathbf{Zn^1Zn//Au^+ \rightarrow ZnZn^{\bullet+}//Au^{\bullet}} \qquad \Delta G^\circ = -0.91 \text{ eV} \quad (1)$$

as shown in the transient absorption experiments below. Rate constants for the forward electron transfer (eq 1) were calculated from the lifetime data and are given in Table 3. The value of ΔG° was calculated using the data in Table 2. The observation of biexponential fluorescence decay traces can be explained by the presence of different conformations of the rotaxanes, due to the flexibility of the macrocycle $\mathbf{Au^+}$ with attached gold porphyrin, in which the ^{1}ZnP−AuP^+ electronic coupling is different (see discussion below). Because we were following the ^{1}ZnP fluorescence, it is clear that it reflected the excited-state decay and not subsequent reactions.

Transient absorption spectra were collected at various time delays after excitation of $\mathbf{Zn_2//Au^+}$ with a 150 fs laser pulse at 575 nm (Figure 7). The spectra show the initial formation of the excited ^{1}ZnP state and the subsequent evolution to the charge-transfer state (eq 1), in agreement with the fluorescence results. Thus, the spectra after 10−100 ps display features of the excited singlet ^{1}ZnP,[25,26,28,31] with a peak at 465 nm and a broad shoulder around 500 nm. Bleaching of the Q(1,0) band can be seen centered around 550 nm, while the Q(0,0) bleaching around 575 nm was covered by stray light from the excitation laser pulses. In the 600−750 nm region, there is a broad absorption, with a bleach feature around 650 nm, due to stimulated ^{1}ZnP emission. The transient spectrum after 500 ps still has some of the typical ^{1}ZnP characteristics, consistent with the fluorescence lifetime data. In contrast, the spectrum after 4700 ps is consistent with that of the charge-transfer state comprising the oxidized $ZnP^{\bullet+}$ and the reduced $AuP^{\bullet}$ radicals.[28,31b,32] For this state, the differential absorption is smaller than that for ^{1}ZnP over the whole spectrum. Furthermore, the peak around 460 nm is slightly blue shifted, the ^{1}ZnP shoulder at 500 nm is absent, and both the stimulated emission at 650 nm and the bleach at 550 nm have disappeared. Instead, a weak absorption from $ZnP^{\bullet+}$ can be seen around 670 nm.

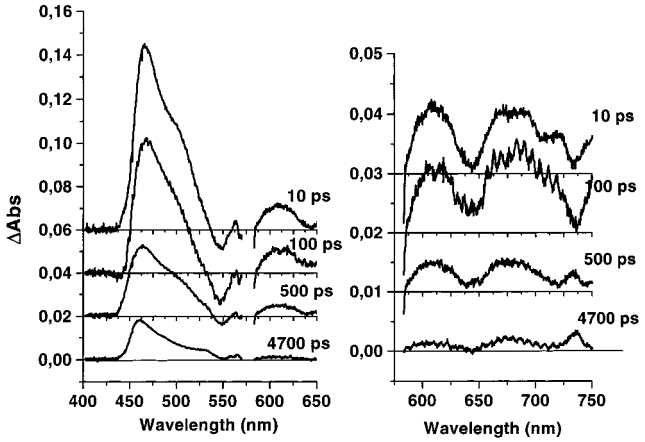

Figure 7. Transient absorption spectra after excitation of the ZnP unit in $\mathbf{Zn_2//Au^+}$ with a 150 fs, 575 nm laser pulse.

The kinetics of the transient absorption decay were studied with various probe light wavelengths in the range 450−650 nm. Figure 8 shows a typical transient trace for $\mathbf{Zn_2//Au^+}$ measured at 460 nm. The excitation pulse induced a strong absorption from the ^{1}ZnP state, that decreased during the first nanosecond as it was converted to the charge-transfer state (eq 1). This is consistent with the ca. 50% smaller extinction coefficient for the $ZnP^{\bullet+}$-$AuP^{\bullet}$ state as compared to that of ^{1}ZnP.[28,32] The charge-transfer state was more long-lived and had decayed only partially after 5 ns, which was the limit of the femtosecond setup. The best fit of the decay curves (Figure 8) was obtained using a triple exponential function.[33] The faster two components corresponded to electron transfer from the ^{1}ZnP state, forming the charge-transfer state (eq 1). The lifetimes obtained, 80 ps (45%) and 570 ps (55%), were in good agreement with the fluorescence decay data. A much slower component, with a

(30) Andréasson, J.; Zetterqvist, H.; Kajanus, J.; Mårtensson, J.; Albinsson, B. *J. Phys. Chem. A* **2000**, *104*, 9307.
(31) (a) Rodriguez, J.; Kirmaier, C.; Holten, D. *J. Am. Chem. Soc.* **1989**, *111*, 6500. (b) Asahi, T.; Ohkohchi, M.; Matsusaka, R.; Mataga, N.; Zhang, R. P.; Osuka, A.; Maruyama, K. *J. Am. Chem. Soc.* **1993**, *115*, 5665.
(32) (a) Neta, P. *J. Phys. Chem.* **1981**, *85*, 3678. (b) Abou-Gamra, Z.; Harriman, A.; *J. Chem. Soc., Faraday Trans. 2* **1986**, *82*, 2337. (c) Fajer, J.; Borg, D. C.; Forman, A.; Dolphin, D.; Felton, R. H. *J. Am. Chem. Soc.* **1970**, *92*, 3451. (d) Shimidzu, T.; Segawa, H.; Iyoda, T.; Honda, K. *J. Chem. Soc., Faraday Trans. 2* **1987**, *83*, 2191. (e) Carnieri, N.; Harriman, H. *Inorg. Chim. Acta* **1982**, *62*, 103. (f) Mosseri, S.; Mialocq, J. C.; Perly, B.; Hambright, P. *J. Phys. Chem.* **1991**, *95*, 2196. (g) Hayes, R. T.; Wasielewski, M. R.; Gosztola, D. *J. Am. Chem. Soc.* **2000**, *122*, 5563. (h) Osuka, A.; Noya, G.; Taniguchi, S.; Okada, T.; Nishimura, Y.; Yamazaki, I.; Mataga, N. *Chem.-Eur. J.* **2000**, *6*, 33.

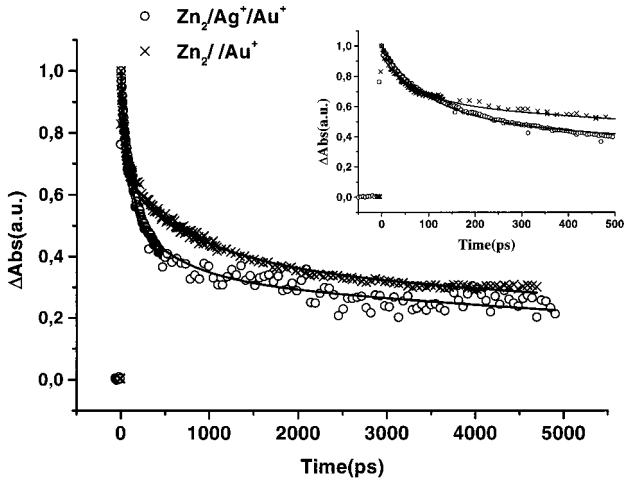

Figure 8. Transient absorption decay at 460 nm for $\mathbf{Zn_2//Au^+}$ and $\mathbf{Zn_2/Ag^+/Au^+}$ after ZnP excitation at 575 nm. The inset shows the decays at early times.

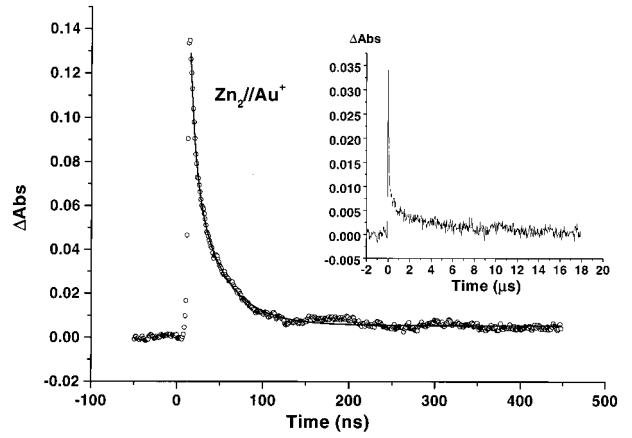

Figure 9. Transient absorption decay at 460 nm for $\mathbf{Zn_2//Au^+}$ on the nano- to microsecond time scale after ZnP excitation at 575 nm with a 5 ns laser pulse.

lifetime of 10 ns, represented back electron transfer from the charge-transfer state, regenerating the ground state:

$$\mathbf{ZnZn^{+\bullet}//Au^{\bullet}} \rightarrow \mathbf{Zn_2//Au^+} \qquad \Delta G^\circ = -1.22 \text{ eV} \quad (2)$$

Using nanosecond flash photolysis, we could follow the complete decay of the transient absorption (Figure 9). A sum of two exponents was needed to fit the data on the nanosecond time scale, giving lifetimes of 10 ns (45%) and 35 ns (55%) for the charge-transfer state. Although the 10 ns component is close to the time resolution limit of the nanosecond setup, the lifetime value is in good agreement with that obtained in the femtosecond experiments. The relative amplitudes of the components show a weight similar to that observed in the forward reaction (eq 1). This suggests that the different rotaxane conformations do not interconvert faster than on the time scale of nanoseconds and that they give different rates also for the back reaction (eq 2).

(33) The following procedure was used to analyze the transient decays on the picosecond time scale; the 570 ps lifetime obtained in the fluorescence lifetime measurements for $\mathbf{Zn_2//Au^+}$ was used as a fixed parameter in the triple exponential fit, while the other lifetimes and all amplitudes were unrestricted. Thus, we obtained lifetimes of 80 ps (45%) and 570 ps (55%) for the forward electron transfer (eq 1), and a much slower decay lifetime of 10 ns corresponding to back electron transfer (eq 2). Note that if instead only the 10 ns component was fixed, the 570 ps lifetime was recovered (±10%), showing the robustness of the fit. The same lifetimes were observed for all probe wavelengths (450−650 nm). Only the relative amplitudes varied in the fit results; either the faster two components, or the slowest one, decreased in amplitude at wavelengths where the corresponding reaction gave small absorption changes.

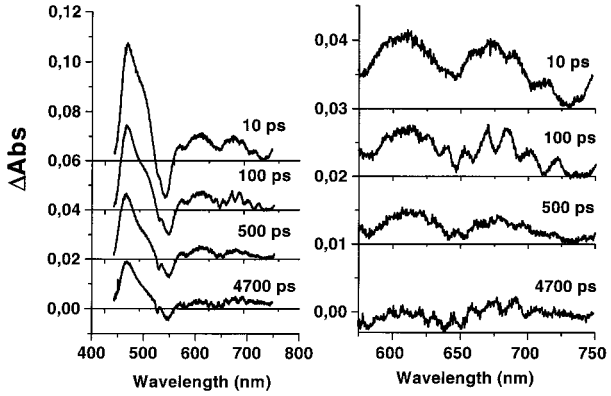

Figure 10. Transient absorption spectra after excitation of the AuP^+ unit in $\mathbf{Zn_2//Au^+}$ with a 150 fs, 528 nm laser pulse.

The triplet quantum yield in porphyrins similar to **Zn** is 0.8−0.9.[25−27] In $\mathbf{Zn_2//Au^+}$ 88.5% of the fluorescence is quenched by electron transfer, leaving 11.5% of the ^{1}ZnP state to decay via the intrinsic pathways. Thus, about 10% of triplet would be formed in competition with electron transfer. The differential extinction coefficient at 460 nm for the triplet is about twice that for the charge-transfer state and would therefore give about 20% of the total signal. Instead, the signal level after the recombination reaction was less than half of that before the recombination (compare initial and final amplitudes in Figure 9) and decayed with a lifetime similar to that for the triplet state of the model **Zn**. Thus, it seems that most of the ^{3}ZnP in $\mathbf{Zn_2//Au^+}$ decayed much faster on a time scale similar to that of the recombination reaction. Electron transfer to the AuP^+ unit is the only conceivable quenching process for the ^{3}ZnP state. Presumably also the ^{3}ZnP state undergoes electron transfer to the AuP^+ unit, but on the same time scale as the subsequent recombination reaction, so that this reaction cannot be resolved. The fraction of $\mathbf{Zn_2//Au^+}$ reacting via the ^{3}ZnP state is too small to account for the full amplitude of either the 10 ns or the 35 ns components in Figure 9. Both of these can be attributed to the recombination reaction, although the ^{3}ZnP decay could contribute to the nanosecond decay signal amplitude.

The reactions in $\mathbf{Zn_2//Au^+}$ are summarized in the scheme of Figure 15. From the fluorescence lifetimes of $\mathbf{Zn_2//Au^+}$ and the model **Zn**, a quantum yield of 85% for charge transfer was calculated. This is also in agreement with the relative magnitudes of the transient absorption changes at 460 nm (Figure 8) where the initial ^{1}ZnP state has about twice the differential extinction coefficient of the $ZnP^{\bullet+}$-$AuP^{\bullet}$ state.[28,32]

Excitation of the AuP^+ Unit. Excitation of the AuP^+ unit generates the $^3AuP^+$ state within a few picoseconds.[25,28,29] The triplet $^3AuP^+$ state displays no emission at room temperature, and the electron-transfer reactions were followed with transient absorption spectroscopy only. Figure 10 shows transient absorption spectra after excitation of $\mathbf{Zn_2//Au^+}$ with 528 nm light. At 10−100 ps, the spectra show characteristic features of the $^3AuP^+$ state[28] with peaks around 460 and 620 nm. After 4700 ps instead, the spectrum has features of the charge-separated state,[28,32] where the shoulder at 500 nm is absent, and the 620 nm signal is much smaller. This shows that electron transfer

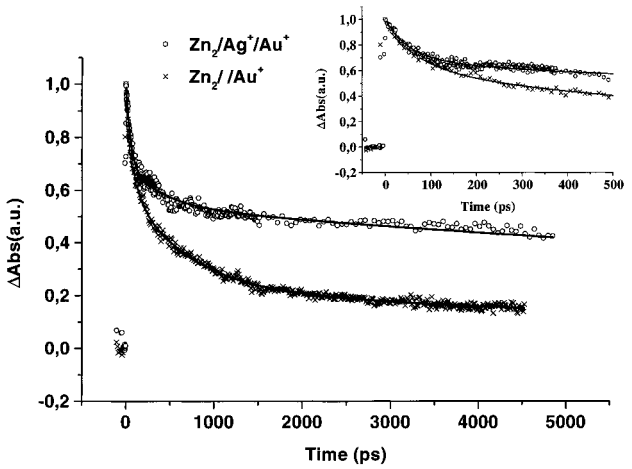

Figure 11. Transient absorption decay at 460 nm for $\mathbf{Zn_2//Au^+}$ and $\mathbf{Zn_2/Ag^+/Au^+}$ after AuP^+ excitation at 528 nm. The inset shows the decay at early times.

from the ZnP to the AuP^+ unit occurred also with AuP^+ excitation:

$$\mathbf{Zn_2//{}^3Au^+ \rightarrow ZnZn^{+\bullet}//Au^\bullet} \qquad \Delta G^\circ = -0.53 \text{ eV} \qquad (3)$$

The transient absorption decay at 460 nm for $\mathbf{Zn_2//Au^+}$ is shown in Figure 11 (together with that of $\mathbf{Zn_2/Ag^+/Au^+}$, see below). As for excitation of the ZnP unit above, the best fit to the decay curves was obtained with a triple exponential function. For $\mathbf{Zn_2//Au^+}$, this gave lifetimes of 90 ps (40%) and 1000 ps (60%), respectively, followed by a slow decay with a lifetime of 10 ns. The transient spectra in Figure 10 display the absorption signature of the $^3AuP^+$ triplet (the shoulder at 500 nm and the peak at 620 nm) also after 500 ps, showing that both of the two faster decay components reflected the forward electron-transfer process (eq 3). The observation of biexponential electron transfer is consistent with the findings for excitation of the ZnP unit above. The different conformations present are likely to give different deactivation rates also for the $^3AuP^+$ triplet.

The 10 ns lifetime of the slowest component is identical to that for the recombination of the charge-transfer state (eq 2) observed after excitation of the ZnP unit. Using nanosecond flash photolysis, the recombination was followed to completion. The transient absorption decay was fitted with a sum of two exponents, giving lifetimes of 10 ns (40%) and 40 ns (60%). The observation of nearly identical recombination lifetimes with excitation of either the ZnP or the AuP^+ unit strongly suggests that the same charge-transfer state is formed, independent of excitation wavelength. Thus, the $ZnP^{\bullet+}$-$AuP^\bullet$ state shows no spin memory of the excited state from which it was formed.

Note that although energy transfer from the $^3AuP^+$ triplet to form the ^3ZnP triplet is energetically possible (Table 2), it cannot explain the transient absorption curves at, for example, 460 nm. The extinction coefficient of the ^3ZnP state is somewhat larger than that of $^3AuP^+$,[28] so that the transient absorption would display a rise rather than a decay. Instead, the data are consistent with electron transfer (eq 3), as the sum of the $ZnP^{\bullet+}$ and $AuP^\bullet$ differential extinction coefficients at 460 nm are approximately one-half of that for the initial $^3AuP^+$ state.[28,32] From the absorption levels in Figure 11, we estimate that the charge-separation yield is about 50%. From the lifetime data instead, we estimate a yield of 65%.

2.3.3. Reactions in $\mathbf{Zn_2/Ag^+/Au^+}$. Excitation of the ZnP Unit. The results for $\mathbf{Zn_2/Ag^+/Au^+}$ obtained with excitation of the ZnP units at 575 nm were quantitatively very similar to those for $\mathbf{Zn_2//Au^+}$. The steady-state fluorescence from the ^{1}-ZnP state in $\mathbf{Zn_2/Ag^+/Au^+}$ was quenched by 74% as compared to that of the model **Zn**. The fluorescence lifetime measurements displayed the same biexponential behavior as for $\mathbf{Zn_2//Au^+}$, with a fast component of 80 ps (31%) and a slower component of 700 ps (66%).[34] Also the transient absorption spectra (not shown) match those for $\mathbf{Zn_2//Au^+}$ in Figure 7.

As for $\mathbf{Zn_2//Au^+}$, the transient absorption kinetics for $\mathbf{Zn_2/Ag^+/Au^+}$ were best fit by a triple exponential function (Figure 8). The fastest two components corresponded to electron transfer from the ^1ZnP state:

$$\mathbf{Zn^1Zn/Ag^+/Au^+ \rightarrow ZnZn^{+\bullet}/Ag^+/Au^\bullet} \qquad \Delta G^\circ = -0.91 \text{ eV} \quad (1')$$

and the lifetimes of 90 ps (40%) and 650 ps (60%) obtained were in good agreement with the emission data. A lifetime of 10 ns was obtained for the third, slower component which was attributed to the recombination reaction:

$$\mathbf{ZnZn^{+\bullet}/Ag^+/Au^\bullet \rightarrow Zn_2/Ag^+/Au^+} \qquad \Delta G^\circ = -1.22 \text{ eV} \quad (2')$$

The recombination was followed to completion using the nanosecond setup, and a biexponential fit to the decays at 460 nm yielded lifetimes of 10 ns (50%) and 40 ns (50%). Thus, the rate constants for both forward and back electron transfer were almost identical in $\mathbf{Zn_2//Au^+}$ and $\mathbf{Zn_2/Ag^+/Au^+}$. Also the yield of charge separation was the same in the two rotaxanes as determined from the 460 nm transient absorption level at the end of the traces in Figure 8. Consequently, we conclude that the presence of the Ag^+ cation has no significant effect on the electron-transfer reactions initiated from the ^1ZnP state. This is in contrast to the effect for the reactions initiated from the $^3AuP^+$ triplet, as discussed below. Note that electron transfer from the ^1ZnP to the $Ag(phen)_2^+$ unit is also energetically possible ($\Delta G^\circ = -0.7$ eV, Table 2). However, since the ^1ZnP lifetime in $\mathbf{Zn_2/Ag^+/Au^+}$ is even slightly longer than that in $\mathbf{Zn_2//Au^+}$, this reaction seems to be insignificant.

As for $\mathbf{Zn_2//Au^+}$ above, the absorption signal remaining after complete decay of the charge-transfer state in the nanosecond experiments was too small to account for the expected fraction of ^3ZnP generated. Thus, it seems that also for $\mathbf{Zn_2/Ag^+/Au^+}$ the ^3ZnP state reacted by electron transfer to the AuP^+ unit on the same time scale as the subsequent recombination.

Excitation of the AuP^+ Unit. Excitation of the AuP^+ unit at 528 nm resulted in transient absorption spectra for $\mathbf{Zn_2/Ag^+/Au^+}$ [13] that were qualitatively identical to those for $\mathbf{Zn_2//Au^+}$ given in Figure 10. The spectra show characteristic features of the $^3AuP^+$ state evolving to the charge-transfer state according to

$$\mathbf{Zn_2/Ag^+/{}^3Au^+ \rightarrow ZnZn^{+\bullet}/Ag^+/Au^\bullet} \qquad \Delta G^\circ = -0.53 \text{ eV} \quad (3')$$

The transient absorption decay at 460 nm is shown in Figure 11. A triple exponential fit gave lifetimes of 50 ps (40%) and

(34) A small fraction (3%) with a lifetime of 2.0 ns was also found, corresponding to the lifetime of the singlet excited state in the model **Zn**.

400 ps (60%), respectively, for the forward electron transfer and 10 ns for the subsequent charge recombination. This should be compared with the forward reaction in $\mathbf{Zn_2//Au^+}$ that gave lifetimes of 90 and 1000 ps (see above). Thus, we note in the case of AuP^+ excitation a clear increase of the electron-transfer rate when the Ag^+ is coordinated to the phenanthroline. This important observation is further supported by the yield of charge transfer. For $\mathbf{Zn_2/Ag^+/Au^+}$, the transient absorption after 3 ns had decayed to 45% of the initial value, suggesting a near unity charge-separation yield. In contrast, we see that the yield for $\mathbf{Zn_2//Au^+}$ was only about one-half of that.

Alternative reactions cannot explain the higher reaction rates in $\mathbf{Zn_2/Ag^+/Au^+}$. Excitation, oxidation, and reduction of the $Ag^+(phen)_2$ unit, as well as energy transfer to form the ^{1}ZnP singlet, can all be ruled out on thermodynamic grounds (Table 2). Energy transfer forming the ^{3}ZnP triplet is exergonic but is not consistent with the transient absorption traces at 460 nm, as discussed for $\mathbf{Zn_2//Au^+}$ above. Finally, the enhanced rate cannot be explained by a simple Ag^+-induced structural change bringing the ZnP and AuP^+ units closer together, since then a faster electron transfer would have been observed also when the ZnP unit was excited. Instead, we propose that coordination of Ag^+ increased the rate of direct electron transfer between the ZnP and AuP^+ units in a superexchange mechanism.[9] In contrast, there was no rate enhancement in $\mathbf{Zn_2/Ag^+/Au^+}$ when the ZnP unit was excited. The Ag^+-induced rate enhancement for electron transfer between the noncovalently linked ZnP and AuP^+ units is one of the main results of the photochemical studies and will be further discussed below.

The charge-separated state decayed with lifetimes of 10 ns (35%) and 40 ns (65%), as determined from the nanosecond flash photolysis traces (not shown). This is very close to the results obtained for $\mathbf{Zn_2//Au^+}$, showing that the recombination reaction was not significantly effected by Ag^+, as was also concluded from the results from ZnP excitation above.

2.3.4. Reactions in $\mathbf{Zn_2/Cu^+/}$. $\mathbf{Zn_2/Cu^+/}$ was studied as a model for the reactions between the ZnP and $Cu(phen)_2^+$ units in $\mathbf{Zn_2/Cu^+/Au^+}$. Excitation of the ZnP units at 575 nm showed that the ^{1}ZnP fluorescence intensity of $\mathbf{Zn_2/Cu^+/}$ was quenched by 90% as compared to that of the model **Zn**. The fluorescence decay of $\mathbf{Zn_2/Cu^+/}$ was single exponential with a lifetime of 180 ps, which corresponds to a 91% quenching as compared to that of the model **Zn**.

In $\mathbf{Zn_2/Cu^+/}$, electron transfer from the singlet ^{1}ZnP to the Cu $(phen)_2^+$ unit is conceivable, but somewhat endergonic (Table 2, Figure 16). This suggests that the emission quenching is instead due to energy transfer to the $Cu(phen)_2^+$ unit, which has an excited state below the ^{1}ZnP state (Table 2). The excited $*Cu(phen)_2^+$, which is probably a singlet and triplet in equilibrium,[35] has an expected lifetime of 175 ns[25,35,36] and is higher in energy than the ^{3}ZnP state (Table 2). Thus, a two-step energy-transfer process is energetically possible (Figure 16):

$$\mathbf{^1ZnZn/Cu^+/ \rightarrow Zn_2/*Cu^+/ \rightarrow {}^3ZnZn/Cu^+/} \qquad (4)$$

The corresponding process was reported by Flamigni et al.[36] in a Zn(II)-porphyrin-stoppered Cu(I) [3]-rotaxane with structural similarities to $\mathbf{Zn_2/Cu^+/}$. Our transient absorption data support the two-step energy-transfer mechanism. The initial transient absorption at 460 nm from ^{1}ZnP decreased rapidly as expected (Figure 12), since the excited $*Cu(phen)_2^+$ absorption is small at this wavelength.[25,35] The subsequent absorption rise up to 90% of the initial level showed that formation of ^{3}ZnP occurred, because this is the only state with an extinction coefficient as high as ^{1}ZnP. A fit according to eq 4 gave a 180 ps lifetime for the ^{1}ZnP state, in excellent agreement with the fluorescence data, and a 650 ps lifetime for the following energy transfer from $*Cu(phen)_2^+$ to ^{3}ZnP. Given the intrinsic lifetimes of ^{1}ZnP and $*Cu(phen)_2^+$, we expect a 90% yield of ^{3}ZnP by the two-step mechanism. Furthermore, since the main competing process is direct intersystem crossing from ^{1}ZnP to ^{3}ZnP we expect a near unity triplet yield. Thus, from the absorption levels in Figure 12, we estimate that the differential extinction coefficient of the ^{3}ZnP state at 460 nm is 90−95% of that for the ^{1}ZnP state. The lifetime of the ^{3}ZnP state was 6 μs, as determined in flash photolysis experiments (not shown), close to the value for the model **Zn**.

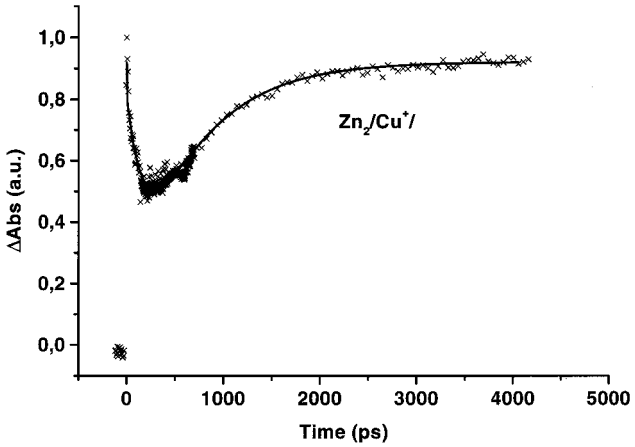

Figure 12. Transient absorption changes at 460 nm for $\mathbf{Zn_2/Cu^+/}$ after ZnP excitation at 575 nm.

2.3.5. Reactions in $\mathbf{Zn_2/Cu^+/Au^+}$. Excitation of the ZnP Unit. Upon excitation at 575 nm, the ^{1}ZnP fluorescence intensity in $\mathbf{Zn_2/Cu^+/Au^+}$ was quenched by 93% as compared to that for the model **Zn**. A double exponential fit to the fluorescence decay curves gave lifetimes of 60 ps (70%) and 300 ps (30%).[37] The fast (60 ps) component was faster than in both $\mathbf{Zn_2/Cu^+/}$ and $\mathbf{Zn_2//Au^+}$, suggesting that energy transfer to $Cu(phen)_2^+$, followed by generation of the ^{3}ZnP state (eq 4″), occurred in competition with electron transfer to the AuP^+ unit (eq 1″):

$$\mathbf{Zn^1Zn/Cu^+/Au^+ \rightarrow ZnZn^{+\bullet}/Cu^+/Au^\bullet} \qquad \Delta G^\circ = -0.91 \text{ eV} \quad (1'')$$

$$\mathbf{Zn^1Zn/Cu^+/Au^+ \rightarrow Zn_2/*Cu^+/Au^+ \rightarrow {}^3ZnZn/Cu^+/Au^+} \qquad (4'')$$

The transient absorption data support this suggestion. This is demonstrated most clearly in the data at 460 nm (Figure 13), where an initial decay of the ^{1}ZnP absorption was followed by a partial recovery as the ^{3}ZnP state was populated, just as for $\mathbf{Zn_2/Cu^+/}$. Because direct electron transfer to the AuP^+ unit

(35) Everly, M. R.; McMillin, D. R. *J. Phys. Chem.* **1991**, *95*, 9071.
(36) Flamigni, L.; Armaroli, N.; Barigelletti, F.; Chambron, J.-C.; Sauvage, J.-P.; Solladie, N. *New J. Chem.* **1999**, *23*, 1151.

(37) The observation of a 300 ps lifetime for the slow conformation in the fluorescence lifetime measurement, that is, a slower ^{1}ZnP decay than that in the $\mathbf{Zn_2/Cu^+/}$, probably reflects the increased uncertainty as the lifetimes of the two conformations become similar and more difficult to deconvolute. The true value is probably ca. 150 ps.

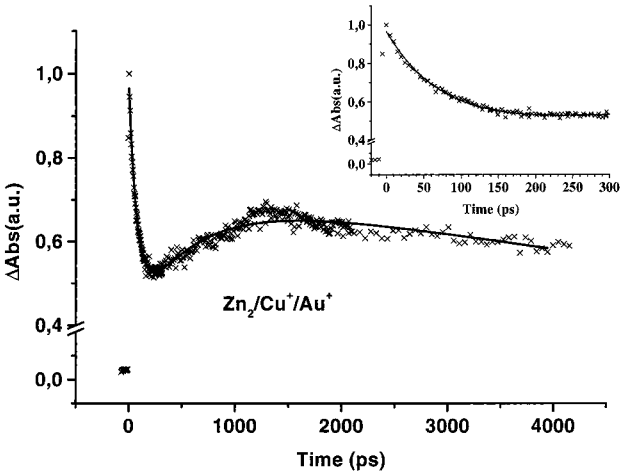

Figure 13. Transient absorption changes at 460 nm for $\mathbf{Zn_2/Cu^+/Au^+}$ after ZnP excitation at 575 nm. The inset shows the decay at early times.

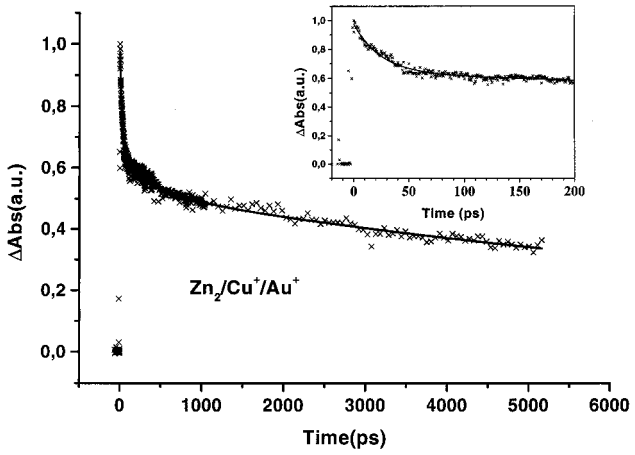

Figure 14. Transient absorption decay at 460 nm for $\mathbf{Zn_2/Cu^+/Au^+}$ after AuP^+ excitation at 528 nm. The inset shows the decay at early times.

competes with the two-step energy transfer, both the ^{3}ZnP and the charge-transfer states were formed on this time scale. Thus, the transient absorption did not recover to the same level in $\mathbf{Zn_2/Cu^+/Au^+}$ as it did in $\mathbf{Zn_2/Cu^+/}$ (compare the signals after ca. 2 ns in Figures 12 and 13). On a slower, nanosecond time scale, the transient absorption decreased again when the charge-separated state recombined to the ground state, as in $\mathbf{Zn_2//Au^+}$.

A fit to the kinetic data[38] gave a lifetime of 55 ps for the initial decay of the ^{1}ZnP state and a 650 ps lifetime for the subsequent rise as the ^{3}ZnP was populated. The 55 ps lifetime of ^{1}ZnP was in good agreement with the fluorescence results and also with the lifetime expected from a combination of the two competing processes, since a 90 ps electron transfer to the AuP^+ unit (as for $\mathbf{Zn_2/Ag^+/Au^+}$) and a 180 ps energy transfer to $Cu(phen)_2^+$ (as in $\mathbf{Zn_2/Cu^+/}$) give an expected ^{1}ZnP lifetime in $\mathbf{Zn_2/Cu^+/Au^+}$ of 60 ps. Thus, the rate of electron transfer from ^{1}ZnP to AuP^+ was apparently unaffected by the presence of Cu^+. The only effect of Cu^+ was consequently to open an additional energy-transfer reaction in parallel to electron transfer. The lifetime data suggest that about two-thirds of the ^{1}ZnP singlet states reacted by electron transfer to the AuP^+ unit, and one-third underwent energy transfer to the $Cu(phen)_2^+$ unit, followed by generation of ^{3}ZnP with $\tau = 650$ ps (eq 4). However, the differential absorption at 460 nm from the charge-transfer and ^{3}ZnP states after 1500 ps was ~0.65 of the initial value (Figure 13), whereas it was ~0.40 for the charge-transfer state in $\mathbf{Zn_2//Au^+}$ (Figure 8). Because the ^{3}ZnP state has twice the extinction coefficient of the charge-transfer state, this indicates that the total fraction of ^{1}ZnP undergoing energy transfer was instead about one-half. The additional ^{3}ZnP generation probably came from the rotaxane conformation that was slow in electron transfer,[37] as seen in the fluorescence decay, although it could not be resolved from the other processes in the transient absorption traces.

The identical rise times of 650 ps obtained in $\mathbf{Zn_2/Cu^+/}$ and $\mathbf{Zn_2/Cu^+/Au^+}$ show that the deactivation of $^*Cu(phen)_2^+$ occurred mainly by energy transfer to ^{3}ZnP, and not by energy and electron transfer to the AuP^+ unit ($\Delta G° = -0.1$and -0.25 eV, respectively). In Figure 16, we present the reaction pathways in $\mathbf{Zn_2/Cu^+/Au^+}$. The reaction scheme proposed is consistent with the transient absorption kinetics over the whole range investigated (450−650 nm) and with the transient spectra (see Figure S2). The most notable difference in the transient spectra as compared to that of the other rotaxanes is that the initial decrease in absorption at 450−520 nm during the first few hundred picoseconds was followed by a recovery that gave a larger signal again after 1000−5000 ps. Similarly, the Q-band bleach at 550 nm grew stronger again after 5000 ps, all consistent with formation of ^{3}ZnP.

The decay of the charge-separated and ^{3}ZnP states was followed by nanosecond flash photolysis. Similar to the case in $\mathbf{Zn_2//Au^+}$ and $\mathbf{Zn_2/Ag^+/Au^+}$ above, the back electron transfer occurred with lifetimes of 10 ns (40%) and 40 ns (60%):

$$\mathbf{ZnZn^{+\bullet}/Cu^+/Au^\bullet \rightarrow Zn_2/Cu^+/Au^+} \qquad \Delta G° = -1.22 \text{ eV} \quad (2'')$$

Thus, the kinetics are unaltered by the insertion of Cu^+ also for the recombination reaction. From the absorption levels at the end of Figure 13, it is clear that the ^{3}ZnP state did not decay significantly within 5 ns. Because its differential extinction coefficient is twice that of the charge-transfer state, the triplet yield estimate above indicates that at least one-half of the signal after 5 ns (at the end of the trace) would be due to the ^{3}ZnP state. However, when the decay of this signal was followed on the nanosecond time scale, the recombination lifetimes of 10 and 40 ns obtained represent 80% of the total nanosecond signal amplitude. Only 20% of the signal decayed with a longer lifetime (ca. 3 μs). This indicates that a large fraction of the ^{3}ZnP states reacted on the time scale of the recombination reaction, and the remaining part reacted much slower. This is again very similar to the case in the other rotaxanes, except that more ^{3}ZnP was generated in $\mathbf{Zn_2/Cu^+/Au^+}$.

Excitation of the AuP^+ Unit. The transient absorption spectra after excitation of $\mathbf{Zn_2/Cu^+/Au^+}$ with 528 nm light were qualitatively the same as for the other rotaxanes, consistent with a $^3AuP^+$ state being converted to the $ZnP^{\bullet+}$-$AuP^\bullet$ state (not shown). Figure 14 shows the transient absorption decay at 460 nm, which was fitted to a triple exponential function as for the other rotaxanes. The faster two components, representing decay of the $^3AuP^+$ state, gave lifetimes of 25 ps (75%) and 470 ps

(38) The kinetic traces were fitted to a stepwise reaction A → B → C, where A is the ^{1}ZnP state, B represents a mixture of the charge-separated state and the excited $^*Cu(phen)_2^+$, and C represents a mixture of the charge-separated state and ^{3}ZnP. A slower exponential decay of the charge-transfer state, fixed to 10 ns according to the flash photolysis results, was also included in the fit. The result was a lifetime of 55 ps for the initial decay (A → B) and 650 ps for the subsequent rise (B → C).

(25%). The third, slower component of 12 ns represented the decay of the charge-transfer state. By nanosecond flash photolysis, this recombination could be followed to completion, giving charge-transfer lifetimes of 12 ns (35%) and 40 ns (65%), close to the values for the other rotaxanes.

The $^3AuP^+$ decay is clearly much faster in $\mathbf{Zn_2/Cu^+/Au^+}$ than in the other rotaxanes. The transient absorption traces show that energy transfer from $^3AuP^+$ cannot explain the higher rates, as discussed for $\mathbf{Zn_2//Au^+}$. Instead, the higher rates can be attributed to a Cu^+-induced enhancement of the rate of electron transfer from ZnP to $^3AuP^+$. This is supported by the resulting transient spectrum that is identical to that for the charge-transfer state in the other rotaxanes. Two different mechanisms for the Cu^+-enhanced electron transfer are possible. Either a bridge-assisted, direct electron transfer from the ZnP to the $^3AuP^+$ unit occurred as in $\mathbf{Zn_2/Ag^+/Au^+}$:

$$\mathbf{Zn_2/Cu^+/{}^3Au^+ \rightarrow ZnZn^{+\bullet}/Cu^+/Au^\bullet} \qquad \Delta G^\circ = -0.53\ \text{eV}\ \ (3'')$$

or the reaction proceeded in a sequential manner via an initial electron transfer from the $Cu(phen)_2^+$ unit to the $^3AuP^+$, followed by a secondary reaction between the ZnP and $Cu(phen)_2^{2+}$ units:

$$\mathbf{Zn_2/Cu^+/{}^3Au^+ \rightarrow Zn_2/Cu^{2+}/Au^\bullet} \qquad \Delta G^\circ = -0.20\ \text{eV} \quad (5)$$

$$\mathbf{Zn_2/Cu^{2+}/Au^\bullet \rightarrow Zn\ Zn^{+\bullet}/Cu^+/Au^\bullet} \qquad \Delta G^\circ = -0.30\ \text{eV}\ \ (6)$$

The fact that the electron-transfer rate is enhanced by Cu^+ shows that $Cu(phen)_2^+$ orbitals are involved in mediating the reaction. However, the energy of the $Cu(phen)_2^{2+}$-$AuP^\bullet$ state is between the energies of the initial $^3AuP^+$ and the final $ZnP^{\bullet+}$-$AuP^\bullet$ state. Consequently, it would rather be formed as a real intermediate according to eqs 5 and 6 than being a virtual state in a superexchange mechanism.[6,9,14] Because the distance between the $Cu(phen)_2^+$ and $^3AuP^+$ units is relatively small, it is likely that the sequential electron transfer may compete with the direct electron-transfer reaction from the ZnP unit. The transient absorption data show no sign of the $Cu(phen)_2^{2+}$-$AuP^\bullet$ intermediate, although this would give a much smaller signal than the final $ZnP^{\bullet+}$-$AuP^\bullet$ state, particularly at 460 nm.[25,32,35] Thus, if the observed decay times of $^3AuP^+$ of 25 and 470 ps reflect the formation of the intermediate according to eq 5, in parallel with the direct electron transfer from the ZnP unit (eq 1″), the subsequent charge transfer to the ZnP unit (eq 6) must be faster than that. This is not unlikely, since the ZnP and $Cu(phen)_2^+$ units are covalently linked via phenyl groups, so that the electronic coupling would be relatively strong.

Note that the relative amplitude of the fastest (25 ps) reaction component is 75%, while it was 40% for $\mathbf{Zn_2//Au^+}$ and $\mathbf{Zn_2/Ag^+/Au^+}$. The components reflect reactions for different rotaxane conformations, and if the same ZnP and $^3AuP^+$ reactants are involved as in the other rotaxanes, the relative amplitudes are not expected to vary. However, the marked difference for $\mathbf{Zn_2/Cu^+/Au^+}$ is consistent with a change to a reaction between the $Cu(phen)_2^+$ and AuP^+ units instead, for which the effect of the different conformations could be quite different. In conclusion, although we have no direct spectral evidence for the formation of the $\mathbf{Zn_2/Cu^{2+}/Au^\bullet}$ state, it seems likely that the electron-transfer mediated by the Cu^+ unit proceeds via the two-step reaction mechanism (eqs 5 and 6).

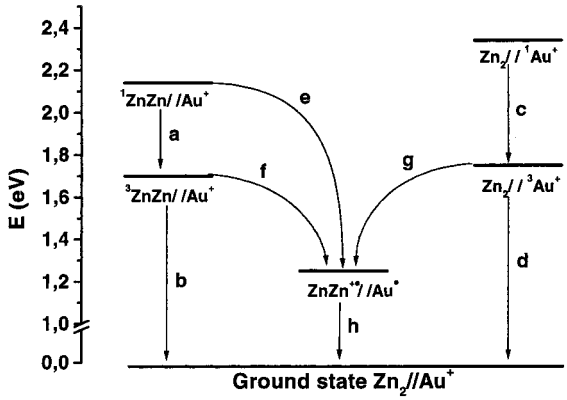

Figure 15. Internal relaxation and electron-transfer processes proposed in $\mathbf{Zn_2//Au^+}$: (a) $k = 5.0 \times 10^8\ s^{-1}$; (b) $k = 1.7 \times 10^5\ s^{-1}$; (c) $k > 3 \times 10^{11}\ s^{-1}$; (d) $k = 2.0 \times 10^8\ s^{-1}$; (e) $k = 1.2 \times 10^{10}\ s^{-1}$ and $1.3 \times 10^9\ s^{-1}$; (f) see text; (g) $k = 1.1 \times 10^{10}\ s^{-1}$ and $5.0 \times 10^8\ s^{-1}$; (h) $k = 1.0 \times 10^8\ s^{-1}$ and $2.9 \times 10^7\ s^{-1}$. The corresponding values for the electron-transfer processes (e−h) $\mathbf{Zn_2/Ag^+/Au^+}$ are (e) $k = 1.2 \times 10^{10}\ s^{-1}$ and $1.1 \times 10^9\ s^{-1}$; (f) see text; (g) $k = 2.0 \times 10^{10}\ s^{-1}$ and $2.0 \times 10^9\ s^{-1}$; (h) $k = 1.0 \times 10^8\ s^{-1}$ and $2.5 \times 10^7\ s^{-1}$.

2.4. General Discussion. We have shown that electron transfer occurs with a lifetime of 100 ps or faster in all the rotaxanes, both from the ^{1}ZnP state to the AuP^+ unit and from the ground-state ZnP to the excited $^3AuP^+$. The same $ZnP^{\bullet+}$-$AuP^\bullet$ charge-transfer state is formed in both cases. This state has a relatively long lifetime, 10−40 ns, giving a ratio of 100 for the forward/backward electron transfer. The charge-transfer state lifetime is much longer than in previous rotaxanes where the ZnP and AuP^+ units were both linked to the rod.[28,39]Despite the weaker coupling in the present case, the charge-separation yield is high, and for $\mathbf{Zn_2/Ag^+/Au^+}$ the yield is >80% irrespective of excitation wavelength. The rate constants for the different processes are given in Figures 15 and 16.

The observation of biexponential electron-transfer kinetics for both the forward and the backward electron transfer may seem puzzling at first. However, the rotaxanes are large and not entirely rigid, and the reactants are not covalently linked to each other. Consequently, one can expect some structural flexibility. The biexponential kinetics may thus be attributed to the presence of different conformations of the rotaxane, which exhibit different donor/acceptor coupling.[40] If the conformational motions occur on the same time scale as electron transfer, or slower, the reaction kinetics will not be single exponential. The data for $\mathbf{Zn_2/Cu^+/}$, where only processes between the ZnP and $Cu(phen)_2^+$ units occur, show single exponential fluorescence decays. Thus, we conclude that the conformation differences

(39) (a) Chambron, J.-C.; Harriman, A.; Heitz, V.; Sauvage, J.-P. *J. Am. Chem. Soc.* **1993**, *115*, 6109. (b) Brun, A. M.; Atherton, S. J.; Harriman, A.; Heitz, V.; Sauvage, J.-P. *J. Am. Chem. Soc.* **1992**, *114*, 4632. (c) Chambron, J.-C.; Harriman, A.; Heitz, V.; Sauvage, J.-P. *J. Am. Chem. Soc.* **1993**, *115*, 7419.

(40) Note that the two different ^{1}ZnP lifetimes we obtain cannot reflect the lifetimes of one of the ZnP units on the same rotaxane reacting faster than the other, since the components do not have a 1:1 amplitude relation, and we see the same biexponential behavior for the $^3AuP^+$ lifetime. Also, the biexponential kinetics cannot be explained by excitation of both ZnP and AuP^+ units in the same experiment. This is shown by the contrasting results obtained for ZnP- and AuP^+-excitation, and the fact that also the ^{1}ZnP fluorescence was biexponential. Finally, the biexponential fluorescence cannot be due to delayed fluorescence (repopulation) since there are no states available close enough in energy to ^{1}ZnP.

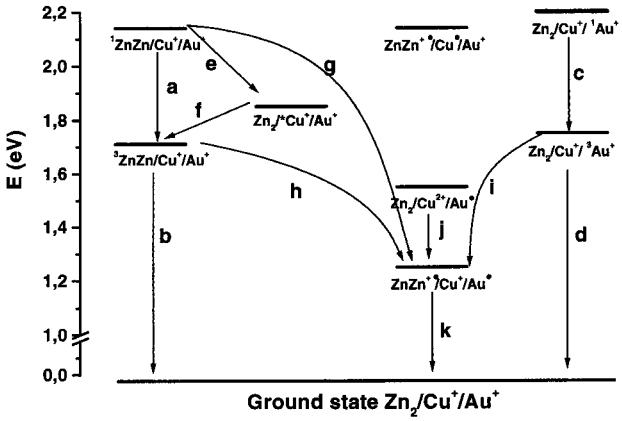

Figure 16. Internal-relaxation, energy-transfer (EnT), and electron-transfer (ET) processes proposed in $\mathbf{Zn_2/Cu^+/Au^+}$. For processes a−d the rate constants are the same as in $\mathbf{Zn_2//Au^+}$: (e) EnT, $k = 5.1 \times 10^9$ s^{-1}; (f) EnT, $k = 1.5 \times 10^9$ s^{-1}; (g) ET, $k = 1.25 \times 10^{10}$ s^{-1}; (h) ET, see text; (i) sequential ET, $k = 3.9 \times 10^{10}$ s^{-1} and 1.6×10^9 s^{-1}; (j) ET, not resolved; (k) ET, $k = 1.0 \times 10^8$ s^{-1} and 2.5×10^7 s^{-1}.

mainly involve motion of the nonrigid $\mathbf{Au^+}$-macrocycle. A rotation of the macrocycle, positioning the AuP^+ between the ZnP units, has been observed in a related rotaxane,[20] but this seems to be excluded in the present case by our NMR data. Furthermore, when Ag^+ or Cu^+ is coordinated so that rotation is prevented, we still observe biexponential kinetics. Instead, twisting and breathing motions of the polyether chain, changing the relative position of the ZnP and AuP^+ units, are plausible origins for the different conformations. Because the recombination reaction was also biexponential, it seems that the conformations do not interconvert faster than on the nanosecond time scale. Note that the rate enhancement due to coordination of Ag^+ or Cu^+ is only observed with AuP^+ excitation and not with ZnP excitation. This shows that it is the through-bond electronic coupling − not through-space − that is important for the reaction. Thus, the different conformations must differ in the through-bond coupling and not just in the through-space ZnP−AuP^+ distance.

For electron-transfer reactions in general, the rate constant (k) decreases exponentially with the distance (d) between the reactants: $k \propto \exp(-\beta d)$, when corrected for the distance dependence of other factors. In a superexchange mechanism,[6,9,14] the parameter β that characterizes the distance dependence of k varies with the nature of the link. It decreases with a decrease in the energy difference between the virtual redox states of the link and the donor/acceptor states. Consequently, saturated hydrocarbon links give relatively large values, $\beta = 0.8-1.0$ Å^{-1},[2a,b] while unsaturated ones give $\beta = 0.2-0.6$ Å^{-1},[2c−f] allowing for rapid long-range electron transfer. Noncovalent bonds and space jumps, however, are believed to be less efficient in mediating electron transfer.[3,6] When the energy of the mediating states of the link approaches that of the donor and acceptor states, a change to a hopping mechanism may occur, in which the link is actually a reduced or oxidized intermediate.[6,7] In that case, the distance dependence is much weaker than that for a superexchange. As an example, charge hopping between guanine bases has recently been shown[8] to explain reports of efficient charge transport over several tens of angströms in DNA.[8,41]

In contrast to many synthetic systems, the rotaxanes of this study have a link comprising different types of bonds, and there is no entirely covalent electron-transfer pathway between the porphyrins. From simple molecular models we estimate a porphyrin edge-to-edge distance of ca. 15−17 Å. Nevertheless, we observed electron-transfer rate constants up to 1.2×10^{10} s^{-1} for a direct reaction between the ZnP and AuP^+ units. This is much faster than for activationless electron transfer in proteins, where a rate constant at 15 Å is typically $<1 \times 10^8$ s^{-1}.[3] In fact, it is comparable to the values obtained in donor/acceptor molecules covalently linked by norbornyl units,[2a] which were found to be more efficient mediators ($\beta = 0.86$ Å^{-1})[2a] than other saturated bonds. In addition, the electron transfer to the $^3AuP^+$ in our rotaxanes is probably not free energy optimized ($\Delta G° = -0.45$ eV), so that an activationless rate constant would be even larger than the value observed here. These comparisons suggest that, although the metal-phenanthroline unit is involved, the electron-transfer pathway may take some shortcuts. A plausible pathway could, for example, involve a direct space jump from the phenanthroline on the rod to the AuP^+ unit, which could come close due to breathing motions of the macrocycle. However, the mediating effect of Ag^+- and Cu^+-coordination upon AuP^+ excitation shows that the ZnP and AuP^+ units did not come close enough for a direct, through-solvent electron transfer, because then the same effect would have been observed with ZnP excitation. Instead, the electron-transfer pathway with AuP^+ excitation involves the metal-phenanthroline complex, which enhances the electronic coupling.

In Table 3, we compare the forward electron-transfer rate constants in the different rotaxanes, and it is clear that coordination of Ag^+ and Cu^+ increases the reaction rate for AuP^+ excitation (eqs 3, 3′, 3″), but not for ZnP excitation (eqs 1, 1′, 1″). The different effect of Ag^+ on the electron-transfer rate, depending on which porphyrin is excited, is very interesting. In both cases the electron is transferred from the ZnP to the AuP^+ unit, and the same charge-separated state is generated. The difference is that the initial excited state is either ^{1}ZnP or $^3AuP^+$. We propose that the results can be explained by considering that different orbitals may be involved in mediating the electronic coupling in the two cases. In Figure 17, we show a schematic picture of HOMO and LUMO orbitals for the ZnP and AuP^+, and the MO:s of the link are represented by only one HOMO/LUMO couple for simplicity. In a superexchange reaction, the donor/acceptor coupling is mediated via a small perturbation by the link.[6,9,14] The mediating contribution from each link unit is inversely proportional to the energy difference (ΔE_n) between the mediating link state and the donor state. Furthermore, the donor/acceptor coupling (H_{AB}) is proportional to the sum of all pairwise transfer integrals (V) between all the states of the link (l_n) and the donor and acceptor: [6,14,42]

$$H_{AB} = \sum V(Al_n)V(Bl_n)/\Delta E_n \qquad (7)$$

As seen in Figure 17, the reaction from ^{1}ZnP is the transfer of an electron from the ZnP LUMO to the AuP^+ LUMO. Because of the proximity in energy, the LUMO:s of the bridge are likely to give the largest contribution to the coupling. This is referred to as the "electron-transfer mechanism"[2b,6,14] since the virtual

(41) (a) Kelley, S. O.; Barton, J. K. *Science* **1999**, *283*, 375. (b) Nunez, M. E.; Hall, D. B.; Barton, J. K. *Chem. Biol.* **1999**, *6*, 85. (c) Murphy, C. J.; Arkin, M. R.; Jenkins, Y.; Ghatlia, N. D.; Bossmann, S. H.; Turro, N. J.; Barton, J. K. *Science* **1993**, *262*, 1025.
(42) May, V.; Kühn, O. *Charge and Energy Transfer Dynamics in Molecular Systems*; Wiley-VCH: Berlin, 2000.

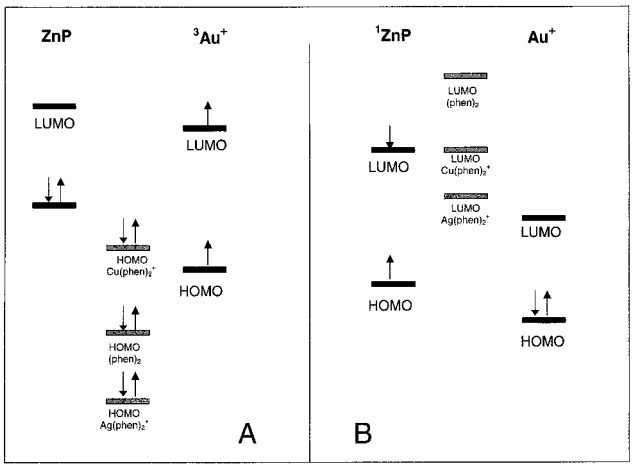

Figure 17. Schematic MO diagram illustrating the effect of bridge energy on through bond electron transfer. (A) Electron transfer from the ground-state ZnP to the $^3AuP^+$ triplet ("hole transfer"). (B) Electron transfer from the singlet ^1ZnP to the ground-state AuP^+ (electron transfer).

intermediate state involved has an additional electron on the link. In the reaction starting with $^3AuP^+$, however, an electron is transferred from the ZnP HOMO to the AuP^+ HOMO. For the same energy proximity reason as before, the bridge HOMO:s will probably give the largest mediating contribution. This is the "hole-transfer mechanism"[2b,6,14] in which the virtual state involves the oxidized link.

The coordination of metal cations changes the energy of the phenanthroline MO:s and introduces new metal-based orbitals. Also, the coupling between the phenanthroline units will be greatly enhanced when they are coordinated to the same metal ion. In the electron-transfer mechanism, starting from ^1ZnP, the LUMO of the $Cu(phen)_2^+$ unit is phenanthroline-based, while $Ag(phen)_2^+$ has low lying unoccupied orbitals on both the metal and the ligand.[43] From the reduction potentials in Table 2, it is clear that the LUMO is stabilized to the same level as that for the ^1ZnP donor state (for Cu^+), or even below (for Ag^+). If the electron-transfer pathway involved the metal-phenanthroline unit, a significant increase in the reaction rate would be expected. Instead, we observed no change, or even a slight decrease with Ag^+. This suggests that the electron-transfer pathway from the ^1ZnP state does not involve these units. For the hole-transfer mechanism instead, starting from $^3AuP^+$, also the phenanthroline HOMO is stabilized by the metal cation, so that the energy difference to the donor state increases. Still, for **Zn_2/Ag^+/Au^+** the electron transfer starting with the $^3AuP^+$ state was faster than for **Zn_2//Au^+**, suggesting that the $Ag(phen)_2^+$ unit mediated the reaction. This apparently contradicting behavior can be explained by the strongly increased coupling between the two phenanthrolines as they become coordinated to the same metal, leading to an increase of the $V(Al_n)V(Bl_n)$ factors in the numerator of eq 7 which compensates for the increase in ΔE_n. In **Zn_2/Cu^+/Au^+**, the $Cu(phen)_2^+$ HOMO is Cu-based, and the redox potentials (Table 2) show that it lies between the donor and acceptor states. This state would therefore not be involved in a superexchange mechanism, but could instead be a real intermediate. Thus, even if there is no direct evidence for the generation of this intermediate (see above), the increased reaction rates show that $Cu(phen)_2^+$ is involved. We therefore suggest that the electron transfer in this case proceeds by a hopping mechanism. A recent study of electron transfer between ZnP and AuP^+ units covalently linked by conjugated hydrocarbon bridges reports a change from superexchange mediation to a hopping mechanism when the energy of the bridge state was gradually decreased.[44] Only electron transfer from ^1ZnP was studied, however, so it is not clear if the mediation behavior with AuP^+ excitation would be different.

Finally, for the recombination reaction of the charge-transfer state, the case is different from both the forward reactions, since an electron should be transferred from the $AuP^\bullet$ LUMO to the $ZnP^{\bullet+}$ HOMO, and all states of the link lie at a very different energy than at least one of these two porphyrin MO:s involved. We observed no effect of Ag^+ or Cu^+ in the experiments, indicating that either the metal-phenanthroline unit was not involved in this reaction or that the changes induced were too small to significantly alter the parameters of eq 7.

To conclude, we propose that the electron transfer following excitation of the AuP^+ unit changes from a superexchange in **Zn_2/Ag^+/Au^+**, which is enhanced as compared to the case in **Zn_2//Au^+**, to a hopping mechanism for **Zn_2/Cu^+/Au^+**, involving the oxidized $Cu(phen)_2^{2+}$ unit as a real intermediate. The effect is a gradual increase in reaction rate throughout the series. In contrast, when the ZnP unit was excited we observed no effect of the coordinated metal cations or even a slight rate decrease. We propose that this can be explained by the different mediating orbitals of the link involved, HOMO for AuP^+ excitation and LUMO for ZnP excitation. This behavior is in contrast to previously reported systems with repeated, identical units of hydrocarbon σ bonds between the reactants, in which a symmetric HOMO/LUMO superexchange mediation was observed.[2b] A mediation asymmetry has been reported for a covalently linked system, in which a synthetic modification of the bridge increased the HOMO-mediated "hole transfer", while no significant effect on the LUMO-mediated "electron transfer" was observed.[45]

3. Conclusions

By selective excitation of either porphyrin, we could follow the electron transfer from the ZnP to the AuP^+ unit in this series of rotaxanes. A rapid, photoinduced electron transfer between the noncovalently linked porphyrins was observed, over an ca. 15−17 Å edge-to-edge distance, with rate constants up to 4×10^{10} s^{-1}. The resulting $ZnP^{\bullet+}$-$AuP^\bullet$ charge-transfer state had a relatively long lifetime, 10−40 ns, and was formed in high yield. For **Zn_2/Ag^+/Au^+** it was >80%, irrespective of excitation wavelength. In **Zn_2/Cu^+/Au^+**, electron transfer to AuP^+ was competing with a two-step energy-transfer process: (i) from ^1ZnP to $Cu(phen)_2^+$ with $k = 5.1 \times 10^9$ s^{-1}, and then (ii) from $^*Cu(phen)_2^+$ to give ^3ZnP with $k = 1.5 \times 10^9$ s^{-1}.

By a simple variation of the linking structure, viz. the coordination of either Ag^+ or Cu^+ to the phenanthroline units, we could enhance the electron-transfer rate from the ZnP to the excited $^3AuP^+$. We interpret our data as a change from a superexchange mechanism for **Zn_2/Ag^+/Au^+**, which is enhanced

(43) (a) Dietrich-Buchecker, C.; Sauvage, J.-P.; Kern, J.-M. *J. Am. Chem. Soc.* **1989**, *111*, 7791. (b) Billon, M.; Divisia-Blohorn, B.; Kern, J.-M.; Sauvage, J.-P. *J. Mater. Chem.* **1997**, *7*, 1169. (c) Schmittel, M.; Ganz, A.; Fenske, D.; Herderich, M. *J. Chem. Soc., Dalton Trans.* **2000**, 353.

(44) Kilså, K.; Kajanus, J.; Macpherson, A. N.; Mårtensson, J.; Albinsson, B. *J. Am. Chem. Soc.* **2001**, *123*, 3069.

(45) Wasielewski, M. R.; Niemczyk, M. P.; Johnson, D. G.; Svec, W. A.; Minsek, D. W. *Tetrahedron* **1989**, *45*, 4785.

as compared to the case in $\mathbf{Zn_2//Au^+}$, to a hopping mechanism for $\mathbf{Zn_2/Cu^+/Au^+}$, involving the oxidized $Cu(phen)_2^{2+}$ unit as a real intermediate. In contrast, electron transfer from the excited ^{1}ZnP to AuP^+ was not affected, or even slowed, by Ag^+ or Cu^+. This asymmetry may possibly be explained by the different orbitals involved in mediating the reaction in an electron- and a hole-transfer mechanism.[6,14] A consideration of the orbital energies involved suggests that also the electron transfer pathway is different dependent on which porphyrin is excited. Our results demonstrate the possibility to tune the rates of electron transfer between the noncovalently linked reactants by a convenient modification of the linking structure. The different effect of Ag^+ and Cu^+ on the rate with ZnP and AuP^+ excitation shows an additional possibility to control the electron-transfer reactions by selective excitation.

4. Experimental Section

Photophysics and Photochemistry. All photophysical measurements were made in spectroscopic grade DMF at 298 K, unless otherwise stated. The samples used for triplet lifetime measurement were deoxygenated by repeated freeze−pump−thaw cycles or by purging with nitrogen gas. The triplet emission spectra were measured in a EtOH/ MeOH 4:1 mixture at 77 K. The ^{1}ZnP state energy of **Zn** was calculated from the midpoint of the absorption and emission peaks (the Q(0,0)-band), while the energy of the nonemitting singlet excited state of $\mathbf{Au^+}$ was calculated from the red end of the lowest absorption peak. The triplet state energies for **Zn** and $\mathbf{Au^+}$ were calculated from the blue edge of the phosphorescence peak at 77 K. The redox potentials are reported as the average between the anodic and cathodic peak potentials. The driving force for the electron-transfer reaction was calculated from the Weller equation:[46] $\Delta G° = zFE^0_{D+/D-} - E^{00}_{D*} - zFE^0_{A/A-} - \Delta w$. The work term ($\Delta w$) is zero for the charge shift reactions between the ZnP and AuP^+ units.

The fluorescence lifetimes were measured with a time correlated single photon counting setup, with an instrumental response function of 80 ps. Excitation pulses at 575 nm (150 fs duration, 200 kHz, <10 nJ/pulse) were delivered an OPA, pumped by a regenerative amplifier/ Ti-sapphire oscillator system. Steady-state emission measurements were made on a Spex Fluorolog spectrometer.

Femtosecond transient absorption measurements were performed using a setup that has been described in detail elsewhere.[47] The pump light is the 150 fs, 1 kHz tunable output of an optical parametric amplifier (TOPAS). The intensity of the pump pulses was kept below 3 μJ to avoid multiple excitation of the same rotaxane. As probe light, a white light continuum created from a 3 mm sapphire window was used. In our experiments, we used an optical delay line that allows a maximum delay of 5 ns relative to the pump light.

In the nanosecond flash photolysis, the following instrumentation was used: a Q-switched Nd:YAG laser (Quantel Brilliant B) pumped an OPO (Opotek) that delivered ca. 5 ns (fwhm) pulses at 528 or 575 nm (ca. 10 nm bandwidth). The pulses were focused in the sample in a standard quartz 1 × 1 cm^2 cell, via a cylindrical lens, giving ca. 15 mJ/pulse excitation light on a 8 × 3 mm^2 spot ($w \times h$). In the flash photolysis spectrometer (Applied Photophysics LKS60), the analyzing light from a pulsed, 150 W xenon lamp was focused in the sample though 2 × 2 mm pinholes, being overlapped by the laser beam in a cross-beam fashion. After the sample, the analyzing light passed a single holographic grating monochromator with two 1−2 mm slits and was focused onto a side-on P928-type PMT. The PMT output was fed into the 50 Ω input of a HP Infinium digital oscilloscope (2 Gs/s) and analyzed using the commercial processor software. At least 10 shots (background and scan) were averaged for each curve. The response time of the whole system, as measured by the rise of an instantaneous absorption increase, was ca. 5 ns (10%−90% rise), and the time jitter between different shots was <1 ns.

Electrochemical Measurements. Cyclic voltammetry measurements were performed with an EG&G Princeton Applied Research potentiostat, model 273A. The working electrode was a Pt disk, the counter electrode was a Pt wire, and a SCE was the reference electrode. The electrolyte was n-Bu_4NPF_6 in dichloromethane.

Synthesis. ^{1}H NMR spectra were obtained on either a Bruker WP 200 SY (200 MHz) or an AM 400 (400 MHz) spectrometer. Chemical shifts in ppm are referenced downfield from tetramethylsilane. Labels of the protons of the [2]-rotaxanes and some of their precursors are provided in Figure 5. Mass spectral data were obtained on either a ZAB-HF (FAB) or a Bruker Protein TOF (MALDI-TOF) spectrometer. Melting points were determined in open capillary tubes on a Büchi SMP-20 apparatus and are uncorrected. Elemental analyses were performed by the "Service de Microanalyse de l'Institut de Chimie de Strasbourg". UV−visible absorption spectra were recorded with a Kontron-Uvikon 860 spectrophotometer.

Schlenk techniques were used for the reactions performed under an atmosphere of argon. Macrocycles **M30**,[15b] $\mathbf{Au^+}$,[18] 2,9-bis-(*p*-formylphenyl)-1,10-phenanthroline **1**,[20] 3,5-di-*tert*-butylbenzaldehyde **2**,[22] and $Cu(CH_3CN)_4PF_6$[19] were prepared according to literature. A procedure for the preparation of (3,3′-dihexyl-4,4′-dimethyl-2,2′-dipyrryl)methane **3** is also given in the Supporting Information.

A. Synthesis of (3,3′-Dihexyl-4,4′-dimethyl-2,2′-dipyrryl)methane 3. This is described in the Supporting Information.

B. Synthesis of [2]-Rotaxanes. Prerotaxane $[/Cu^+/Au^+](PF_6^-)_2$. A degassed solution of $Cu(CH_3CN)_4{\cdot}BF_4$ (0.0342 g; 0.11 mmol) in CH_3CN (10 mL) was added via cannula to a solution of macrocycle $\mathbf{Au^+}$ (0.200 g; 0.11 mmol) in dry CH_2Cl_2 (20 mL). After stirring for 20 min, a solution of 2,9-bis-(*p*-formylphenyl)-1,10-phenanthroline (0.042 g; 0.11 mmol) in dry CH_2Cl_2 was added via cannula to the solution of the complex formed. After stirring for 2 h, the mixture was treated with a saturated aqueous solution of KPF_6. The organic layer was extracted and evaporated to dryness to give pure $\mathbf{[/Cu^+/Au^+](PF_6^-)_2}$ (0.264 g; 0.11 mmol; 100%) as a red solid. ^{1}H NMR (400 MHz, CD_2Cl_2): δ 9.69 (s, 2H, C*H*O); 9.44 (d, 2H, H_{py1}, ^3J = 5.3 Hz); 9.32 (s, 4H, $H_{py3+py4}$); 9.29 (d, 2H, H_{py2}, ^3J = 5.3 Hz); 8.94 (d, 2H, $H_{4',7'}$, ^3J = 8.4 Hz); 8.46 (s, 2H, $H_{5',6'}$); 8.43 (d, 2H, $H_{4,7}$, ^3J = 8.4 Hz); 8.11 (d, 2H, $H_{3',8'}$, ^3J = 8.4 Hz); 8.06 (d, 4H, H_{op1}, ^4J = 1.7 Hz); 7.92 (t, 1H, H_{pp2}, ^4J = 1.7 Hz); 7.91 (d, 2H, $H_{3,8}$, ^3J = 8.4 Hz); 7.90 (d, 2H, H_{op2}, ^4J = 2.0 Hz); 7.84 (s, 2H, $H_{5,6}$); 7.84 (t, 2H, H_{pp1}, ^4J = 1.7 Hz); 7.67 (d, 4H, $H_{o'}$, ^3J = 8.1 Hz); 7.59 (d, 2H, H_{op3}, ^4J = 2.0 Hz); 7.22 (d, 4H, H_o, ^3J = 8.9 Hz); 7.33 (t, 1H, H_{pp3} , ^4J = 2.0 Hz); 7.12 (d, 4H, $H_{m'}$, ^3J = 8.1 Hz); 6.12 (d, 4H, H_m, ^3J = 8.9 Hz); 4.46 (m, 4H, H_δ); 4.07 (m, 4H, H_γ); 3.84 (m, 8H, $H_{\alpha+\beta}$); 1.53 (s, 18H, H_{tBu2}); 1.49 (s, 36H, H_{tBu1}). FAB-MS: m/z = 2279.9 [$\mathbf{M} - PF_6^-$]$^+$, calcd 2279.87, 25%; 2134.5 [$\mathbf{M} - 2PF_6^- + e^-$]$^+$, calcd 2134.91, 20%; 1746.0 [$\mathbf{Au^+} + Cu^+ + e^-$]$^+$, calcd 1746.43, 95%; 1682.8 [$\mathbf{Au^+}$], calcd 1682.94, 100%; 1069.6 [$\mathbf{M} - 2PF_6^-$]$^{2+}$/2, calcd 1067.45, 84%; 873.3 [$\mathbf{Au^+} + Cu^+$]$^{2+}$/2, calcd 873.0, 95%.

[2]-Rotaxane $\mathbf{[(H_2)_2/Cu^+/Au^+](PF_6^-)_2}$. Prerotaxane $\mathbf{[/Cu^+/Au^+](PF_6^-)_2}$ (0.264 g; 0.11 mmol), 3,5-di-*tert*-butylbenzaldehyde (0.190 g; 0.87 mmol), and **3** (0.345 g; 1.1 mmol) were dissolved in dry CH_2Cl_2 (100 mL) under argon. Trifluoroacetic acid (four drops) was then added, and the mixture was stirred at room temperature for 16 h. Subsequently, chloranil (tetrachloro-*p*-benzoquinone) (0.800 g; 3.27 mmol) was added, and the reaction mixture was refluxed for 1.5 h. After neutralization by $NaHCO_3$, the organic layer was washed three times with water, treated with a saturated aqueous solution of KPF_6, and then evaporated to dryness. The crude product was purified by repeated column chromatography on silicagel (eluent: CH_2Cl_2/0.5% MeOH) and on alumina (eluent: CH_2Cl_2) affording pure $\mathbf{[(H_2)_2/Cu^+/Au^+](PF_6^-)_2}$ (0.081 g; 0.02 mmol; 18% yield) as a red solid. ^{1}H NMR (400 MHz,

(46) Rehm, O.; Weller, A. *Ber. Bunsen-Ges. Phys. Chem.* **1969**, *73*, 834.
(47) Andersson, M.; Davidsson, J.; Hammarström, L.; Korppi-Tommola, J.; Peltola, T. *J. Phys. Chem. B* **1999**, *103*, 3258.

CD_2Cl_2): δ 10.16 (s, 4H, H_{meso}); 9.55 (d, 2H, H_{py1}, $^3J = 5.1$ Hz); 9.45 (d, 2H, H_{py2}, $^3J = 5.5$ Hz); 9.39 (d, 2H, H_{py3}, $^3J = 5.4$ Hz); 9.35 (d, 2H, H_{py4}, $^3J = 5.4$ Hz); 9.21 (d, 2H, $H_{4',7'}$, $^3J = 8.5$ Hz); 8.86 (s, 2H, $H_{5',6'}$); 8.52 (d, 2H, $H_{3',8'}$, $^3J = 8.4$ Hz); 8.32 (d, 2H, $H_{4,7}$, $^3J = 8.1$ Hz); 8.14 (d, 4H, H_{op1}, $^4J = 1.8$ Hz); 8.10 (d, 2H, H_{op2}, $^4J = 1.8$ Hz); 8.07 (d, 4H, $H_{o'}$, $^3J = 8.4$ Hz); 8.06 (d, 2H, $H_{3,8}$, $^3J = 8.4$ Hz); 7.98 (t, 3H, $H_{pp1+pp2}$, $^4J = 1.6$ Hz); 7.88 (d, 4H, $H_{op'}$, $^4J = 1.8$ Hz); 7.84 (t, 2H, $H_{pp'}$, $^4J = 1.8$ Hz); 7.63 (d, 2H, H_{op3}, $^4J = 2.2$ Hz); 7.60 (d, 4H, H_o, $^3J = 8.4$ Hz); 7.54 (s, 2H, $H_{5,6}$); 7.46 (d, 4H, $H_{m'}$, $^3J = 8.1$ Hz); 7.21 (t, 1H, H_{pp3}); 6.33 (d, 4H, H_m, $^3J = 8.4$ Hz); 4.44 (m, 4H, H_δ); 4.24 (m, 4H, H_γ); 4.08 (m, 16H, $H_{\alpha+\beta+\alpha'2}$); ~3.9 (m, 8H, $H_{\alpha'1}$); 2.45 (s, 12H, H_{Me2}); ~2.2 (m, 8H, $H_{\beta'2}$); 2.08 (m, 8H, $H_{\beta'1}$); 1.78 (s, 12H, H_{Me1}); ~1.7 (m, 16H, $H_{\gamma'1+\gamma'2}$); 1.53 (s, 36H, H_{tBu1}); 1.52 (s, 18H, H_{tBu2}); 1.47 (s, 36H, $H_{tBu'}$); ~1.3 (m, 32H, $H_{\delta'1+\delta'2+\epsilon'1+\epsilon'2}$); 0.8 (m, 24H, $H_{Me\ hex}$); −2.57 (s, 2H, N*H*); −2.67 (s, 2H, N*H*). FAB-MS: $m/z = 4002.1$ [**M** − PF_6^-]$^+$, calcd 4002.7, 26%; 3856.8 [**M** − $2PF_6^-$ + e^-]$^+$, calcd 3857.7, 44%; 2173.4 [**M** − $2PF_6^-$ − **Au**$^+$]$^+$, calcd 2174.7, 24%; 1928.4 [**M** − $2PF_6^-$]$^{2+}$/2, calcd 1928.9, 100%; 1682.8 [**Au**$^+$], calcd 1682.9, 68%. UV−visible (CH_2Cl_2), λ, nm (ϵ, M^{-1} cm^{-1}): 416 (762 000); 511 (43 600); 543 (18 300); 574 (15 800); 626 (2300).

[2]-Rotaxane [Zn_2/Cu^+/Au^+](PF_6^-)$_2$. A solution of **[$(H_2)_2$/Cu^+/Au^+](PF_6^-)$_2$** (0.065 g; 0.016 mmol) and $Zn(OAc)_2 \cdot 2H_2O$ (0.032 mmol) in a mixture of $CHCl_3$ (20 mL) and MeOH (10 mL) was refluxed under argon for 1 h. After evaporation of the solvent, the residue was taken up in CH_2Cl_2, washed twice with water, and evaporated. The crude product was purified by column chromatography on alumina (eluent: CH_2Cl_2) to leave pure **[Zn_2/Cu^+/Au^+](PF_6^-)$_2$** (0.055 g; 0.013 mmol; 82%) as a red solid. ^{1}H NMR (400 MHz, CD_2Cl_2): δ 10.12 (s, 4H, H_{meso}); 9.56 (d, 2H, H_{py1}, $^3J = 5.5$ Hz); 9.45 (d, 2H, H_{py2}, $^3J = 5.2$ Hz); 9.37 (d, 2H, H_{py3}, $^3J = 5.2$ Hz); 9.35 (d, 2H, H_{py4}, $^3J = 5.1$ Hz); 9.27 (d, 2H, $H_{4',7'}$, $^3J = 8.6$ Hz); 8.86 (s, 2H, $H_{5',6'}$); 8.54 (d, 2H, $H_{3',8'}$, $^3J = 8.2$ Hz); 8.26 (d, 2H, $H_{4,7}$, $^3J = 8.2$ Hz); 8.16 (d, 4H, H_{op1}, $^4J = 2.1$ Hz); 8.11 (d, 2H, H_{op2}, $^4J = 1.7$ Hz); 8.07 (d, 4H, $H_{o'}$, $^3J = 8.2$ Hz); 8.04 (d, 2H, $H_{3,8}$, $^3J = 8.2$ Hz); 7.95 (t, 3H, $H_{pp1+pp2}$); 7.90 (d, 4H, $H_{op'}$, $^4J = 1.7$ Hz); 7.81 (t, 2H, $H_{pp'}$, $^4J = 1.7$ Hz); 7.67 (d, 2H, H_{op3}, $^4J = 2.4$ Hz); 7.58 (d, 4H, H_o, $^3J = 8.6$ Hz); 7.55 (s, 2H, $H_{5,6}$); 7.47 (d, 4H, $H_{m'}$, $^3J = 9.0$ Hz); 7.20 (t, 1H, H_{pp3}); 6.35 (d, 4H, H_m, $^3J = 8.6$ Hz); 4.46 (m, 4H, H_δ); 4.11 (m, 4H, H_γ); 4.08 (m, 16H, $H_{\alpha+\beta+\alpha'2}$); ~3.97 (m, 8H, $H_{\alpha'1}$); 2.42 (s, 12H, H_{Me2}); ~2.15 (m, 8H, $H_{\beta'2}$); 2.05 (m, 8H, $H_{\beta'1}$); 1.76 (s, 12H, H_{Me1}); ~1.68 (m, 16H, $H_{\gamma'1+\gamma'2}$); 1.52 (s, 36H, H_{tBu1}); 1.50 (s, 18H, H_{tBu2}); 1.49 (s, 36H, $H_{tBu'}$); ~1.3 (m, 32H, $H_{\delta'1+\delta'2+\epsilon'1+\epsilon'2}$); 0.89 (t, 12H, $H_{Me2\ hex}$, $^3J = 7.2$ Hz); 0.89 (t, 12H, $H_{Me1\ hex}$, $^3J = 7.2$ Hz). FAB-MS: $m/z = 4128.8$ [**M** − PF_6^-]$^+$, calcd 4129.4, 51%; 3983.1 [**M** − $2PF_6^-$ + e^-]$^+$, calcd 3984.5, 54%; 2300.0 [**M** − $2PF_6^-$ − **Au**$^+$]$^+$, calcd 2301.5, 25%; 2238.7 [**M** − $2PF_6^-$ − **Au**$^+$ − Cu^+ + H^+]$^+$, calcd 2238.98, 13%; 1991.6 [**M** − $2PF_6^-$]$^{2+}$/2, calcd 1992.2, 52%; 1745.2 [**Au**$^+$ + Cu^+ + e^-]$^+$, calcd 1682.9, 91%; 1684.4 [**Au**$^+$], calcd 1682.9, 91%. UV−visible (CH_2Cl_2), λ, nm (ϵ, M^{-1} cm^{-1}): 415 (890 000); 538 (44 300); 574 (19 600).

[2]-Rotaxane [Zn_2//Au^+](PF_6^-)$_2$. A solution of rotaxane **[Zn_2/Cu^+/Au^+](PF_6^-)$_2$** (0.030 g; 0.007 mmol) and KCN (22 mg; 0.35 mmol) in a mixture of $CHCl_3/H_2O/CH_3CN$, 1/1/4 (3 mL), was heated at 40 °C for 30 min. Solvents were evaporated, and the residue was taken-up in CH_2Cl_2. The organic layer was washed twice with water, treated with a saturated aqueous solution of KPF_6, and evaporated to dryness. The crude product was purified by column chromatography on alumina (eluent: hexane/CH_2Cl_2, 50/50) affording pure **[Zn_2//Au^+](PF_6^-)$_2$** and some starting material, which was subjected to the same reaction conditions again. This procedure was repeated five times. The overall yield after a total of five reactions was 92%. **[Zn_2//Au^+](PF_6^-)$_2$** (0.026 mg; 0.0063 mmol), red solid. ^{1}H NMR (400 MHz, CD_2Cl_2): δ 10.03 (s, 4H, H_{meso}); 9.48 (d, 8H, $H_{o'}$, $^3J = 8.1$ Hz); 9.42 (d, 2H, H_{py1}, $^3J = 5.1$ Hz); 9.36 (d, 2H, H_{py3}, $^3J = 5.1$ Hz); 9.34 (d, 2H, H_{py4}, $^3J = 5.1$ Hz); 9.24 (d, 2H, H_{py2}, $^3J = 5.1$ Hz); 8.90 (d, 2H, $H_{3',8'}$, $^3J = 8.4$ Hz); 8.63 (d, 4H, H_o, $^3J = 8.7$ Hz); 8.57 (d, 2H, $H_{4',7'}$, $^3J = 8.4$ Hz); 8.08 (d, 2H, H_{op2}, $^3J = 1.8$ Hz); 8.03 (d, 4H, H_{op1}, $^3J = 1.8$ Hz); 7.99 (t, 1H, H_{pp2}, $^3J = 1.8$ Hz); 7.98 (s, 2H, $H_{5',6'}$); 7.92 (t, 2H, H_{pp1}, $^3J = 1.8$ Hz); 7.86 (t, 1H, H_{pp3}, $^3J = 1.8$ Hz); 7.84 (d, 4H, $H_{op'}$, $^3J = 1.8$ Hz); 7.80 (t, 2H, $H_{pp'}$, $^3J = 1.8$ Hz); 7.72 (d, 4H, $H_{m'}$, $^3J = 8.1$ Hz); 7.70 (t, 2H, H_{op3}, $^3J = 1.8$ Hz); 7.53 (d, 2H, $H_{3,8}$, $^3J = 8.4$ Hz); 7.00 (d, 4H, H_m, $^3J = 9.0$ Hz); 6.72 (d, 2H, $H_{4,7}$, $3J = 8.4$ Hz); 4.85 (s, 2H, $H_{5,6}$); 4.44 (m, 4H, H_δ); 4.10 (m, 4H, H_α); 4.01 (m, 4H, H_γ); ~3.9 (m, 8H, $H_{\alpha'2}$); 3.85 (m, 4H, H_β); 3.75 (m, 8H, $H_{\alpha'1}$); 2.38 (s, 12H, H_{Me2}); ~2.1 (m, 8H, $H_{\beta'2}$); 2.03 (s, 12H, H_{Me1}); ~2.0 (m, 8H, $H_{\beta'1}$); ~1.7 (m, 16H, $H_{\gamma'1+\gamma'2}$); 1.52 (s, 18H, H_{tBu2}); 1.47 (s, 36H, H_{tBu1}); 1.46 (s, 36H, $H_{tBu'}$); ~1.3 (m, 32H, $H_{\delta'1+\delta'2+\epsilon'1+\epsilon'2}$); 0.9 (m, 24H, $H_{Me\ hex}$). FAB-MS: $m/z = 3920.4$, [**M** − PF_6]$^+$, calcd 3920.9, 70%; 2238.3, [**M** − $2PF_6^-$ − **Au**$^+$ − Cu^+ + H^+]$^+$, calcd 2238.98, 22%; 1960.4, [**M** − PF_6^- − e^-]$^{2+}$/2, calcd 1960.5, 16%; 1682.4, [**Au**]$^+$, calcd 1682.94, 100%. UV−visible (CH_2Cl_2), λ, nm (ϵ, M^{-1} cm^{-1}): 414 (870 000); 538 (39 300); 574 (16 500).

[2]-Rotaxane [Zn_2/Ag^+/Au^+](PF_6^-)$_2$. To a solution of **[Zn_2//Au^+](PF_6^-)$_2$** (0.004 g; 9.8×10^{-4} mmol) in dry CH_2Cl_2 was added under argon, via syringe, a solution of $AgBF_4$ (0.75 mL of a 1.5×10^{-3} M solution, 1.2×10^{-6} mmol) in CH_3CN. After stirring the solution for 1 h, the solvents were evaporated. The residue was taken-up in CH_2Cl_2, washed with water, and treated by an aqueous solution of KPF_6. The crude product was purified by column chromatography on alumina (eluent: CH_2Cl_2) giving pure **[Zn_2/Ag^+/Au^+](PF_6^-)$_2$** (0.004 g, 9.7×10^{-4} mmol, 99%) as a red solid. ^{1}H NMR (400 MHz, CD_2Cl_2): δ 10.09 (s, 4H, H_{meso}); 9.54 (d, 2H, H_{py1}, $^3J = 5.2$ Hz); 9.44 (d, 2H, H_{py2}, $^3J = 5.2$ Hz); 9.38 (d, 2H, $H_{4',7'}$, $^3J = 8.2$ Hz); 9.37 (s, 4H, $H_{py3+py4}$); 8.77 (s, 2H, $H_{5',6'}$); 8.58 (d, 2H, $H_{3',8'}$, $^3J = 7.9$ Hz); 8.14 (d, 2H, $H_{4,7}$, $^3J = 7.9$ Hz); 8.13 (d, 4H, H_{op1}, $^4J = 1.8$ Hz); 8.10 (d, 2H, H_{op2}, $^4J = 1.8$ Hz); 8.09 (d, 4H, $H_{o'}$, $^3J = 7.9$ Hz); 7.98 (m, 3H, $H_{pp1+pp2}$); 7.87 (d, 4H, $H_{op'}$, $^4J = 1.9$ Hz); 7.84 (t, 2H, $H_{pp'}$, $^4J = 1.8$ Hz); 7.76 (d, 4H, H_o, $^3J = 8.6$ Hz); 7.62 (d, 2H, H_{op3}, $^4J = 2.1$ Hz); 7.54 (d, 4H, $H_{m'}$, $^3J = 8.2$ Hz); 7.52 (d, 2H, $H_{3,8}$, $^3J = 8.2$ Hz); 7.33 (s, 2H, $H_{5,6}$); 7.16 (t, 1H, H_{pp3}, $^4J = 2.1$ Hz); 6.45 (d, 4H, H_m, $^3J = 8.6$ Hz); 4.36 (m, 4H, H_δ), 4.02 (m, 4H, H_γ); ~3.9 (m, 12H, $H_{\beta+\alpha'2}$); 3.87 (m, 4H, H_α); 3.70 (t, 8H, $H_{\alpha'1}$, $^3J = 7.8$ Hz); 2.42 (s, 12H, H_{Me2}); ~2.2 (m, 8H, $H_{\beta'2}$); 1.94 (m, 8H, $H_{\beta'1}$); 1.7 (s, 12H, H_{Me1}); ~1.7 (m, 16H, $H_{\gamma'1+\gamma'2}$); 1.54 (s, 36H, H_{tBu1}); 1.50 (s, 18H, H_{tBu2}); 1.49 (s, 36H, $H_{tBu'}$); ~1.4 (m, 32H, $H_{\delta'1+\delta'2+\epsilon'1+\epsilon'2}$); 0.8 (t, 12H, $H_{Me\ hex}$). FAB-MS: $m/z = 4173.1$ [**M** − PF_6^-]$^+$, calcd 4173.7, 43%; 4027.4 [**M** − $2PF_6^-$ + e^-]$^+$, calcd 4028.8, 46%; 2344.6 [**M** − $2PF_6^-$ − **Au**$^+$ − Ag^+ + H^+]$^+$, calcd 2345.8, 22%; 2236.7 [**M** − $2PF_6^-$ − **Au**$^+$]$^+$, calcd 2237.9, 17%; 2013.5 [**M** − $2PF_6^-$]$^{2+}$/2, calcd 2014.4, 41%; 1789.4 [**Au**$^+$ + Ag^+ + e^-]$^+$, calcd 1790.8, 35%; 1682.1 [**Au**]$^+$, calcd 1682.9, 100%. UV−visible (CH_2Cl_2), λ, nm (ϵ, M^{-1} cm^{-1}): 415 (884 000); 538 (42 200); 574 (17 000).

[2]-Rotaxane [Zn_2/Li^+/Au^+](PF_6^-)$_2$. To a solution of **[Zn_2//Au^+](PF_6^-)$_2$** (0.009 g; 2.2×10^{-3} mmol) in dry CH_2Cl_2 was added, under argon, a solution of $LiBF_4$ in MeOH (0.7 mL of a 6.3×10^{-3} M, 4.4 10^{-3} mmol) via syringe. The solution was stirred for 2 h. The solvents were evaporated, leaving pure **[Zn_2/Li^+/Au^+](PF_6^-)$_2$** (0.009 g; 2.2×10^{-3} mmol; 100%) as a red solid. ^{1}H NMR (400 MHz, CD_2Cl_2): δ 10.11 (s, 4H, H_{meso}); 9.56 (d, 2H, H_{py1}, $^3J = 5.2$ Hz); 9.45 (d, 2H, H_{py2}, $^3J = 5.2$ Hz); 9.37 (s, 2H, $H_{py3+py4}$); 9.21 (d, 2H, $H_{4',7'}$, $^3J = 8.6$ Hz); 8.89 (s, 2H, $H_{5',6'}$); 8.48 (d, 2H, $H_{3',8'}$, $^3J = 8.5$ Hz); 8.23 (d, 2H, $H_{4,7}$, $^3J = 8.2$ Hz); 8.13 (d, 4H, H_{op1}, $^4J = 1.8$ Hz); 8.12 (d, 2H, $H_{3,8}$, $^3J = 8.2$ Hz); 8.10 (d, 2H, H_{op2}, $^4J = 1.8$ Hz); 7.98 (m, 3H, $H_{pp1+pp2}$); 7.97 (d, 4H, $H_{o'}$, $^3J = 8.0$ Hz); 7.88 (d, 4H, $H_{op'}$, $^4J = 1.8$ Hz); 7.86 (m, 2H, $H_{pp'}$); 7.63 (d, 2H, H_{op3}, $^4J = 2.1$ Hz); 7.58 (d, 4H, H_o, $^3J = 8.8$ Hz); 7.44 (d, 4H, $H_{m'}$, $^3J = 8.0$ Hz); 7.39 (s, 2H, $H_{5,6}$); 7.19 (t, 1H, H_{pp3}, $^4J = 2.4$ Hz); 6.36 (d, 4H, H_m, $^3J = 8.6$ Hz); 4.42 (m, 4H, H_δ); 4.06 (m, 4H, H_γ); 3.99 (m, 4H, H_β); 3.92 (m, 12H, $H_{\alpha+\alpha'2}$); 3.78 (m, 8H, $H_{\alpha'1}$); 2.41 (s, 12H, H_{Me2}); ~2.15 (m, 8H, $H_{\beta'2}$); 2.04 (m, 8H, $H_{\beta'1}$); 1.75 (s, 12H, H_{Me1}); ~1.7 (m, 16H, $H_{\gamma'1+\gamma'2}$); 1.53 (s, 18H, H_{tBu2}); 1.52 (s, 36H, H_{tBu1}); 1.48 (s, 36H, $H_{tBu'}$); ~1.3 (m, 32H, $H_{\delta'1+\delta'2+\epsilon'1+\epsilon'2}$); 0.85 (t, 12H, $H_{Me\ hex}$). ^{7}Li NMR (400 MHz, $CDCl_3$/LiCl, D_2O): δ 2.79 (s). UV−visible (CH_2Cl_2), λ, nm (ϵ, M^{-1} cm^{-1}): 415 (878 000); 538 (37 400); 574 (16 700).

Scheme 1

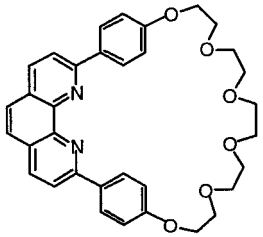

M30

C. Synthesis of [2]-Rotaxane [Zn_2/Cu^+/](PF_6^-)$_2$. Prerotaxane [/Cu^+/](PF_6^-)$_2$. The synthesis of this molecule was achieved using the same experimental conditions as for the prerotaxane **[/Cu^+/Au^+](PF_6^-)$_2$**, with the following quantities: solution of macrocycle **M30** (0.100 g; 0.17 mmol) in CH_2Cl_2 (5 mL), solution of $[Cu(CH_3CN)_4]PF_6$ (0.66 g; 0,18 mmol) in CH_3CN (3 mL), and solution of 2,9-bis-(*p*-formylphenyl)-1,10-phenanthroline (0.068 g; 0.17 mmol) in CH_2Cl_2 (5 mL). **[/Cu^+/](PF_6^-)$_2$** was obtained quantitatively as a red-brown solid (Scheme 1).[48]

[2]-Rotaxane [Zn_2/Cu^+/](PF_6^-)$_2$. The synthesis of this molecule was achieved using the same experimental conditions as for the prerotaxane **[(H_2)$_2$/Cu^+/Au^+](PF_6^-)$_2$**, with the following quantities: **[/Cu^+/](PF_6^-)$_2$** (0.195 g, 0.17 mmol), **3** (0.538 g; 1.70 mmol), 3,5-di-*tert*-butylbenzaldehyde (0.296 g; 1.36 mmol), and CH_2Cl_2 (100 mL). After workup, the crude intermediate **[(H_2)$_2$/Cu^+/](PF_6^-)$_2$** was metalated with $Zn(OAc)_2 \cdot 2H_2O$, using the same experimental conditions as for [2]-rotaxane **[Zn_2/Cu^+/Au^+](PF_6^-)$_2$**. ^{1}H NMR (400 MHz, CD_2Cl_2): δ 10.18 (s, 4H, H_{meso}); 9.07 (d, 2H, $H_{4',7'}$, ^3J = 8.5 Hz); 8.57 (s, 2H, $H_{5',6'}$); 8.42 (d, 2H, $H_{3',8'}$, ^3J = 8.3 Hz), 8.36 (d, 2H, $H_{4,7}$, ^3J = 8.3 Hz); 8.10 (d, 2H, $H_{3,8}$, ^3J = 8.3 Hz); 8.03 (d, 4H, $H_{o'}$, ^3J = 8.1 Hz); 7.89 (d, 4H, $H_{op'}$, ^4J = 1.8 Hz); 7.86 (t, 2H, $H_{pp'}$, ^3J = 1.7 Hz); 7.55 (d, 4H, H_o,^3J = 8.8 Hz); 7.53 (s, 2H, $H_{5,6}$); 7.44 (d, 4H, $H_{m'}$, ^3J = 8.1 Hz); 6.24 (d, 4H, H_m, ^3J = 8.6 Hz); 3.92 (s, 4H, H_ϵ); ~3.75 (m, 32H, $H_{\alpha'1+\alpha'2+\alpha+\beta+\gamma+\delta}$); 2.47 (s, 12H, H_{Me2}); ~2.13 (m, 16H, $H_{\beta'1+\beta'2}$); 1.81 (s, 12H, H_{Me1}); ~1.53 (m, 48H, $H_{\gamma'1+\gamma'2+\delta'1+\delta'2+\epsilon'1+\epsilon'2}$); 1.51 (s, 36H, $H_{tBu'}$); 0.89 (t, 24H, $H_{Me\ hex}$, J = 7.1 Hz).

Acknowledgment. We thank J. Korppi-Tommola for the loan of an optical delay line, R. Hueber for the FAB mass spectra, and J.-D. Sauer and M. Martigneaux for the high-field NMR spectra. Support from the European TMR program (network contract CT96-0031), the Wallenberg Foundation, and the Swedish Research Council for Engineering Sciences is gratefully acknowledged. M.L. thanks the French Ministry of Science for a fellowship.

Supporting Information Available: Pyrrole and dipyrromethane synthesis description, cyclic voltammograms of **Zn**, **Au**$^+$, and **Zn_2/Cu^+/Au^+**, ground-state absorption spectra of **Zn** and **Au**$^+$, and transient absorption spectra for **Zn_2/Cu^+/Au^+** after excitation of the AuP^+ unit (PDF). This material is available free of charge via the Internet at http://pubs.acs.org.

JA0119907

(48) Chambron, J.-C.; Heitz, V.; Sauvage, J.-P. *Bull. Soc. Chim. Fr*. **1995**, *132*, 340.